CLASS 3 CUSTOMER DESIGNATED DISTRIBUTION

HANDBOOK ON FLAW EVALUATION WATERFORD UNIT 3 REACTOR VESSEL OUTLET NOZZLE TO SHELL WELDS

May, 1988

W. H. Bamford
Y. S. Lee
K. R. Balkey
R. D. Rishel
D. Kurek
G. Wendell

Verified By C. Bradley Bond
C. B. Bond

Approved By S. S. Palusamy/SSP
S. S. Palusamy, Manager
Structural Materials Engineering

WESTINGHOUSE ELECTRIC CORPORATION
POWER SYSTEMS
P.O. BOX 355
PITTSBURGH, PA 15230

TABLE OF CONTENTS

TABLE OF CONTENTS (Cont'd.)

EXECUTIVE SUMMARY

This report was prepared as a result of the discovery of indications in the reactor vessel outlet nozzle to vessel weld during the inservice inspection of Spring 1988. The body of the report provides the backgound and technical basis for the construction of a flaw evaluation chart for indications in the outer region of the nozzle to shell weld. The detailed results of the Spring 1988 inspection and the results of application of this flaw chart are found in Appendix A. The report has been structured in this way so that the flaw evaluation chart may be used for future inspections as well.

The results of the inspection showed three indications that exceeded the standards tables of Section XI, IWB-3500, and which therefore required fracture evaluation. These indications have all been plottted on the chart in Figure A-18, and were found thereby to be acceptable without repair.

SECTION 1
INTRODUCTION

This flaw* evaluation handbook has been designed for the evaluation of indications that may be discovered during inservice inspection of the Waterford Unit 3 reactor vessel outlet nozzle to vessel weld region. The geometry of this region is shown in Figure 1-1. The tables and charts provided herein allow the evaluation of any indication discovered in the reactor vessel nozzle to sheli region without further fracture mechanics calculations. The fracture analysis work is documented in this report. Use of the handbook will allow the acceptability (by analysis) of larger indications than would be allowable by only using the standards tables of the ASME Code Section XI. This report also provides the background and technical basis for the handbook charts. This handbook was prepared as a result of the discovery of indications in the reactor vessel outlet nozzle to shell weld near the outer surface in spring of 1988. Details of these indications and their evaluation are contained in Appendix A.

The highlight of the handbook is the design of a series of flaw evaluation charts for embedded flaws in this region. The flaw evaluation charts were designed based on the Section XI code criteria of acceptance (by analysis) for continued service without repair. Through use of the charts, a flaw can be evaluated by code criteria instantaneously, and no follow-up hand calculation is required. Most important of all, no fracture mechanics knowledge is needed by the user of the handbook charts.

It is important to note that indications which are large enough to exceed the standards limits, and must be evaluated by fracture mechanics, will also require additional inservice inspection in the future, as discussed in Section XI, paragraph IWB-2420[1]**.

*The use of the term "flaw" in this document should be taken to be synonymous with the term "indication" as used in Section XI of the ASME Code.
**Numbers in brackets are references in Section 6.

1.1 CODE ACCEPTANCE CRITERIA

There are two alternative sets of flaw acceptance criteria for continued service without repair in paragraph IWB-3600 of ASME Code Section XI [1]. Namely,

1. Acceptance Criteria Based on Flaw Size (IWB-3611)
2. Acceptance Criteria Based on Stress Intensity Factor (IWB-3612)

The choice of criteria is at the convenience of the user, per IWB-3610. Both criteria are comparable in accuracy for thick sections, and the acceptance criteria (2) have been assessed by past experience to be generally less restrictive for thin sections. In all cases, the most beneficial criteria have been used, generally criteria (2).

1.1.1 CRITERIA BASED ON FLAW SIZE

The code acceptance criteria stated in IWB-3611 of Section XI are:

$a_f < .1\, a_c$ For normal conditions (upset & test conditions inclusive)

and $a_f < .5\, a_i$ For faulted conditions (emergency condition inclusive)

where

a_f = The maximum size to which the detected flaw is calculated to grow in a specified time period, which can be the next scheduled inspection of the component, or until the end of vessel design lifetime.

a_c = The minimum critical flaw size under normal operating conditions (upset and test conditions inclusive)

a_i = The minimum critical flaw size for initiation of nonarresting growth under postulated faulted conditions. (emergency conditions inclusive)

To determine whether a flaw is acceptable for continued service without repair, both criteria must be met simultaneously. Accordingly, both criteria have been considered in advance before the charts were constructed. Only the most restrictive results were used in the charts.

1.1.2 CRITERIA BASED ON STRESS INTENSITY FACTOR

As mentioned in the preceding paragraphs, the criteria used for the construction of the charts in this handbook are from the least restrictive of IWB-3611 or IWB-3612 of Section XI. The criteria in IWB-3612 are based on safety margins between the applied stress intensity factor and the fracture toughness of the material.

The term stress intensity factor (K_I) is defined as the driving force on a crack. It is a function of the size of the crack and the applied stresses, as well as the overall geometry of the structure. In contrast, the fracture toughness (K_{Ia}, K_{Ic}) is a measure of the resistance of the material to propagation of a crack. It is a material property, and varies as a function of temperature.

The criteria are stated in IWB-3612:

$$K_I < \frac{K_{Ia}}{\sqrt{10}}$$ For normal conditions (upset & test conditions inclusive)

$$K_I < \frac{K_{Ic}}{\sqrt{2}}$$ For faulted conditions (emergency conditions inclusive)

where

K_I = The maximum applied stress intensity factor for the flaw size a_f to which a detected flaw will grow, for a specified time period, which must equal or exceed the time until the next inspection.

K_{Ia} = Fracture toughness based on crack arrest for the corresponding crack tip temperature.

K_{Ic} = Fracture toughness based on fracture initiation for the corresponding crack tip temperature.

To determine whether a flaw is acceptable for continued service without repair, both criteria for normal and faulted conditions must be met simultaneously. Accordingly, both criteria have been considered in advance before the charts were constructed. Only the most restrictive results (for either normal or faulted conditions) were used in the charts.

1.1.3 PRIMARY STRESS LIMITS

In addition to satisfying the fracture criteria, it is required that the primary stress limits of Section III, paragraph NB 3000 be satisfied. A local area reduction of the pressure retaining membrane must be used, equal to the area of the indication, and the stresses increased to reflect the smaller cross section. All the flaw acceptance tables provided in this handbook have included this consideration, as demonstrated herein. The allowable flaw depth "a" determined using this criterion is 2.31 in. for a continuous longitudinal surface flaw in the reactor vessel nozzle to shell region, and for a continuous circumferential surface flaw the allowable depth "a" is 7.61 inches. Thus the fracture mechanics criteria are governing.

1.2 GEOMETRY

The geometry of the reactor vessel outlet nozzle to shell region of the Waterford Unit 3 reactor vessel is shown in figure 1-1. The dimensions shown are the minimum values from the design drawings. For purposes of heat transfer, the outside surfaces have been assumed to be insulated. The notation used for flaws in this work is illustrated in figure 1-2.

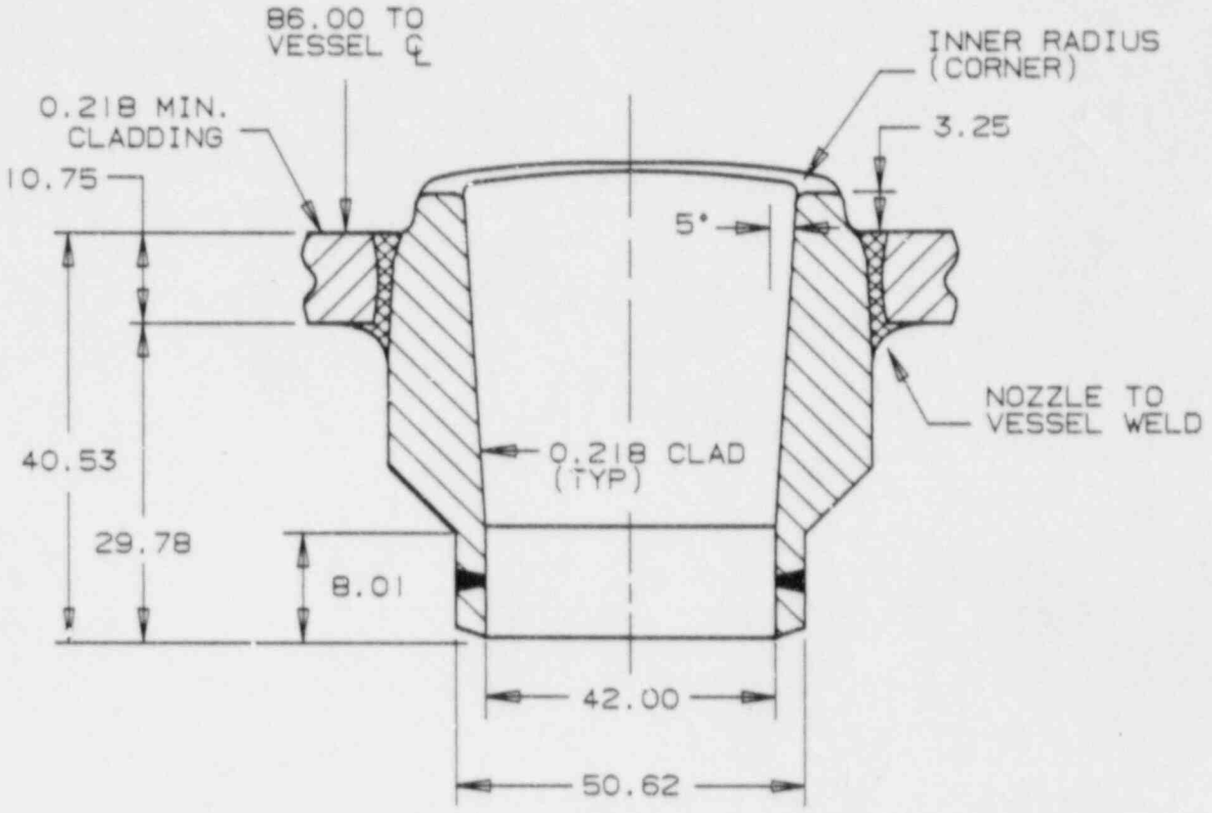

NOTES:

1. DIMENSIONS DO NOT INCLUDE CLAD
2. ALL DIMENSIONS ARE IN INCHES

047-A-25903-1

Figure 1-1. Geometry of Reactor Vessel Outlet Nozzle to Shell Region for Waterford Unit 3

Note: All dimensions in inches.

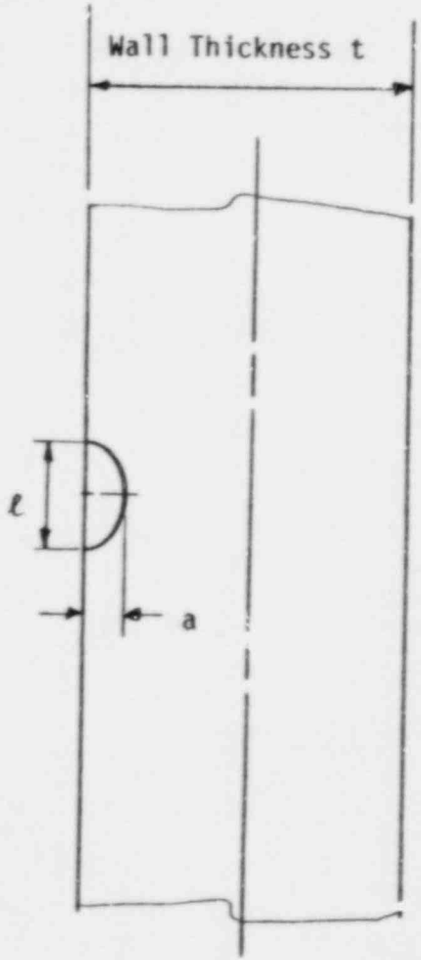

TYPICAL SURFACE FLAW INDICATION

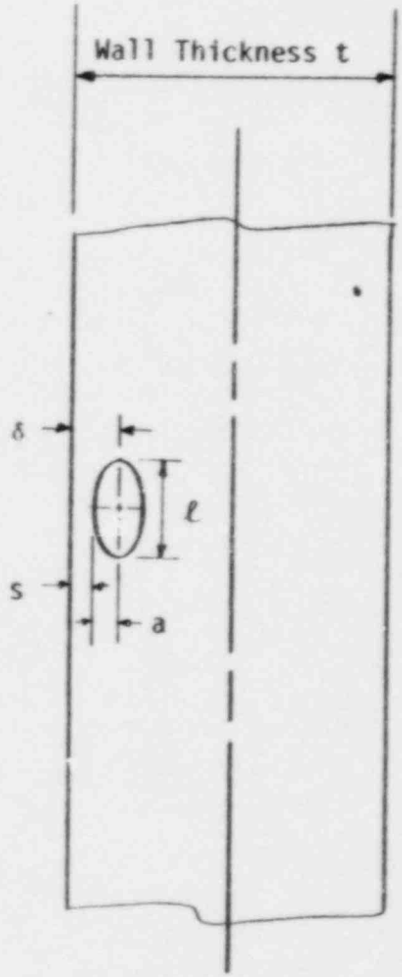

TYPICAL EMBEDED FLAW INDICATION

Figure 1-2 Typical Notation for Surface and Embedded Flaw Indications

SECTION 2
LOAD CONDITIONS, FRACTURE ANALYSIS METHODS AND MATERIAL PROPERTIES

2.1 DETERMINATION OF LIMITING TRANSIENTS

The design and operating transients for the Waterford Unit 3 reactor vessel are listed in table 2-1. Both the minimum critical flaw sizes, such as a_c under normal operating conditions, or a_i under faulted conditions for criteria (1) of IWB-3611, and the allowable stress intensity factors, K_I, for criteria (2) of IWB-3612, are a function of the stresses at the cross-section where the flaw of interest is located, and the material properties. Therefore, the first step for the evaluation of a flaw indication is to determine the appropriate limiting load conditions for the location of interest.

For the region of interest, the reactor vessel nozzle to shell weld, the full range of design transients was considered. The governing emergency and faulted condition transient requires extensive study, in light of the large number of transient scenarios that emerged with the pressurized thermal shock issue. Because the indications have been found near the outside surface of the vessel, the thermal shock transients will generally produce compressive stresses in the region of the indications.

2.1.1 Normal and Upset Conditions

The most severe of the normal, upset and test conditions in the outer region of the outlet nozzle to shell weld was found to be the cold hydrotest condition [2,3], a constant temperature pressure test, generally carried out at the beginning of plant life. For indications at or near the outside surface, all the other transients of table 2-1 are less severe, because no pressure exceeds the 3105 psi used for the hydrotest, and thermal transients will always result in compressive or near zero stresses near the outside

surface of the vessel. The only transient which does result in tensile stresses in this region is the heatup event, but the tensile stresses are very small.

2.1.2 Emergency and Faulted Conditions

The full set of emergency and faulted transients were considered here. All these transients involve severe cooling of the inside vessel surface, which results in compressive loadings near the outer surface. The overcooling events which also involve pressure loadings are therefore the only ones of interest, because without pressure the stresses in the vicinity of the indications would be entirely compressive. Although a very large number of scenarios were considered in the treatment of the pressurized thermal shock issue [4], the key categories of events can be summarized succinctly, as was done in the recent evaluation of Calvert Cliffs [5]. These transients are listed in Table 2-1. The Calvert Cliffs plant was chosen as the representative generic plant for the pressurized thermal shock issue, so the transients of Table 2-1 were assumed to be representative of events for Waterford as well. Detailed stress and fracture results are not available for all of these transients for the Waterford plant, but since the area of interest is the outside surface and near-surface region of the nozzle to shell junction, the following approach was adopted.

The pressure and temperature transients for each of the events from table 2-1 are available in references 4 and 5. They range from moderate to severe cooldowns, and many have severe repressurizations up to the relief valve setting of 2500 psi. To encompass the entire range of transients as they affect the outer surface region of the nozzle to shell weld, the maximum pressure case was chosen for analysis. Since some cases involve a severe thermal shock, and some only a minor thermal shock, the level of compressive thermal stress in the region of interest ranges accordingly from large to small. It is therefore conservative to neglect the compressive thermal stress altogether, and use only the maximum pressure. Because the location of interest is deep in the vessel wall, and the outer surface is insulated, the temperature will always be sufficient for the fracture toughness to be on the

upper shelf. In fact, because RT_{NDT} is 0°F or lower for the materials here (see section 2.3), the material temperature could be as low as 100°F and the material would still be on the upper shelf.

Therefore, the maximum pressure case was evaluated for the governing faulted condition. Transients that can involve repressurization to the maximum pressure (relief valve set point) include many of the large steamline break events, and some of the small steamline breaks.

A separate case was also considered, that of a low temperature overpressure event, as will be discussed below. No additional fracture analysis was necessary for this event, since the worst case event of 1100 psi at a temperature of 110°F is not as severe as the governing PTS event evaluated. This transient is the event experienced by Turkey Point Unit 4 in November 1981.

2.1.3 Treatment of Low Temperature Overpressurization Transients (LTOP)

In this section, the frequency of occurrence of a significant low temperature overpressurization (LTOP) challenge to the Waterford-3 plant is calculated. For this calculation, a probabilistic risk assessment model is used. The model is based on event tree analysis which defines the possible event scenarios that may lead to a significant LTOP challenge for the nuclear plant. This work demonstrates that an LTOP event is of such a low probability that it may be classified as a faulted condition.

Model Assumptions

The PRA model is constructed on the basis of the following assumptions:

1. The LTOP event is of concern if the reactor coolant temperature is less tnan 350 degrees F.

2. There are written operational procedures for overpressurization mitigation. The operators are trained in mitigating the LTOP event.

3. During cooldown, the Shutdown Cooling System (SDCS) safety relief valves are placed in service between 350 and 285 degrees F, while a steam bubble remains in the pressurizer. After the SDCS safety relief valves are placed in service at less than 350 degrees F., the reactor coolant system is cooled and taken solid after reaching 200 degrees F. The time required to remove decay heat to 135°F is approximately 27.5 hours.

4. Normal operating procedures maximize the use of a pressurizer cushion (steam bubble) during periods of low temperature operation. A steam bubble is formed in the pressurizer at a cold leg temperature below 200°F when the plant is being started up. It is collapsed at a cold leg temperature below 200°F when the plant is being cooled down.

   This cushion substantially reduces the severity of some potential transients, such as reactor coolant pump induced heat input and slows the rate of pressure rise for others. This provides reasonable assurance that most potential transients can be terminated by operator action before an overpressure condition exists.

5. The SCDS safety relief valves can not be in maintenance during LTOP.

6. A reactor coolant pump shall not be started when the reactor coolant system temperature is less than the minimum temperature for the inservice pressure test unless either:

   There is a pressure absorbing volume in the pressurizer,

   -or-

   The secondary water temperature of each steam generator is less than 100 degrees F. above the temperature of the reactor coolant system.

7. A control room alarm provides an indication to the operator of any overpressure transient occurring which causes the reactor coolant system pressure to exceed 392 psia.

8. The motor operated and hydraulic-pneumatic valves upstream of the SDCS safety relief valves can close both safety relief valve trains from either a spurious closure, or a false high pressure input signal. The general surveillance time interval of 12 hours will be assumed for these valves.

9. The failure rate for a sensor (2.8E-06/hr) includes all failure modes (i.e., incorrect signal no signal or spurious signal). Since a spurious signal makes up a very small percent of this number, a conservative value of 2.8E-07/hr will be used for the present calculation. This assumes that 1 out of 10 sensor failures are spurious signals.

Event Tree Analysis

Event tree analysis is used to model and quantify the progression and frequency of significant LTOP challenges. The event tree considers the following six items in the progression of a significant LTOP challenge:

1. An LTOP precursor challenges the plant safety systems as an initiating event. This challenge may be due to inadvertent addition of heat or mass into the reactor coolant system, e.g. in the form of startup of a reactor coolant pump or a safety injection pump, or due to blockage of letdown lines.

2. Reactor coolant temperature during the challenge is below 350 degrees F. If not, the LTOP event is not a concern.

3. The SDCS safety relief valves are available. This system is available if one or two of the safety relief valve trains are available.

4. The pressurizer has bubble formation. If the bubble exists, operator action is possible even if both SDCS safety relief valve trains fail.

5. High pressure alarms and valves operate. If they do, the operator can take manual action. Operator action is only credible if a bubble is present. Otherwise, the event progresses too fast for operator response.

6. Operator mitigates the event. This is credible if the bubble is present in the pressurizer and the alarms function.

Success Criteria

The success criteria to avoid a significant LTOP event is either of the following:

At least one mitigating system (SDCS) safety relief valve train is available.

-or-

If both of the mitigation system (SDCS) safety relief valve trains fail, then there must be a bubble in the pressurizer and the alarm must function and the operator action must be successful.

Data Used

Two sets of data were used for the calculation of the frequency of a significant LTOP event. The first set was a best estimate calculation; the second one was a conservative estimate calculation.

1. Initiating event frequency. (Event tree node OPC)

   In the absence of plant specific data for initiating event frequency, an estimate of one challenge per calendar year is made. As a conservative value, twice that value, or two challenges per calendar year will be used.

2. Reactor coolant temperature during the challenge is less than 350 degrees F. (Event tree node TMP)

The probability of the temperature being in the range of concern is unknown. It will be taken as 0.9, assuming that challenge occurs 90 percent of the time in the temperature range of concern. The same value will be used for the conservative estimate.

3. Overpressure protection is available.(Event tree node OPS)

The unavailability of each SCDS safety relief valve train upon demand is as follows:

SDCS safety relief valve fails to open on demand = 3.0E-04

Motor operated isolation valve spuriously closes = (12/2 + (27.5)) (1.0E-07) = 3.4E-06

Hydraulic-pneumatic valve spuriously closes = (12/2 + (27.5)) (1.37E-06) = 4.6E-05

One of two redundant hydraulic solenoid vent valves spuriously open = (12/2 + (27.5)) (1.10E-07) 2 = 7.4E-06

Total unavailability per SDCS safety relief valve train = 3.6E-04

The probability of any one of the two SDCS safety relief valve trains being unavailable is (3.6E-04) 2 = 7.2E-04

The probability of SDCS safety relief valve trains unavailability (both trains unavailable) is calculated as follows:

q = random failure of both SDCS safety relief valve trains + random failure of both pressure sensors + failure of both pressure sensors by common cause + failure of both SDCS safety relief valve trains due to common cause.

The random failure of a sensor is = ((12/2 + (27.5)) (2.8E-07) = 9.4E-06

The common cause value is calculated using the beta factor method. A beta factor of 0.10 is assumed.

The calculation is then:

$$q = (3.6E\text{-}04)^2 + (9.4E\text{-}06)^2 + (0.10)\ (9.4E\text{-}06) + (0.10)\ (3.6E\text{-}04)$$
$$q = 3.7E\text{-}05$$

4. The pressurizer has a bubble formation.(Event tree node WSO)

   It will be assumed that there is no bubble in 80 percent of the challenges. This is due to operational practices in which the bubble is formed after heat-up, and the reactor coolant system is taken solid after reaching 200 degrees F during cooldown. The same value will also be used for the conservative estimate.

5. High pressure and SDCS safety relief valve isolation valve closure alarms work. (Event tree node ALR)

   It will be assumed that the failure of these alarms occurs once in one hundred challenges. This is considered to be conservative.

6. Operator mitigates the event. (Event tree node OPA)

   The operator failure probability to respond to the alarm within a five minute period may be taken as 0.01, assuming that there are at least two operators in the control room and the alarm works; and there is a bubble formation in the reactor coolant system, giving the operators a three to ten minute response time. However, as a conservative estimate an operator failure probability of 1.0 will be used.

Data Summary

The following data were used to quantify the event tree for best estimate and conservative estimate scenarios for the frequency of a significant LTOP challenge per calendar year:

	BEST ESTIMATE	CONSERVATIVE
Initiating event frequency	1.0	2.0
Reactor coolant temp. is less than 350 F.	0.90	0.90
Overpressure protection (SDCS) availability:		
Both SCDS safety relief valve trains are available	0.9924	0.9924
Only one SDCS safety relief valve train is available	7.2E-04	7.2E-04
Both SDCS safety relief valve trains are unavailable	3.7E-05	3.7E-05
No bubble in the pressurizer	0.80	0.80
Alarm fails	0.01	0.01
Operator fails to mitigate		
Alarm works/bubble available	1.0	1.0
Alarm fails	1.0	1.0
Bubble not available	1.0	1.0

Calculations and Conclusions

The event trees in tables 2-2 and 2-3 are used to calculate the frequency of a significant LTOP event per calendar year for the Waterford-3 plant as follows:

The best estimate frequency is 3.4E-05 per calendar year.

The conservative estimate frequency is 6.6E-05 per calender year.

Note that these estimates are based upon a surveillance time interval of 12 hours and an LTOP exposure of 27.5 hours. The time period used for calculation of components having an hourly failure rate (12/2 + 27.5) is 33.5 hours. Increasing the exposure to LTOP by a factor of 10, to 275 hours or 11 days, will increase the best estimate frequency by approximately a factor of 2.3.

Based on the above results, the frequency of a significant LTOP event is very low for the Waterford-3 plant. According to the event categorization rules of ANS and the NRC regulatory guide 1.48, Table 2-4, this LTOP event is clearly classified as a faulted condition. This event was not a governing transient for the flaw evaluation charts because it is much less severe than the other faulted conditions.

2.2 STRESS INTENSITY FACTOR CALCULATIONS

One of the key elements of the critical flaw size calculations is the determination of the driving force or stress intensity factor (K_I). This was done using expressions available from the literature. In all cases the stress intensity factor for the critical flaw size calculations utilized a representation of the actual stress profile rather than a linearization. This was necessary to provide the most accurate determination possible of the critical flaw size, and is particularly important for consideration of emergency and faulted conditions, where the stress profile is generally nonlinear and often very steep. The stress profile was represented by a cubic polynomial:

$$\sigma(x) = A_0 + A_1 \frac{x}{t} + A_2 \left(\frac{x}{t}\right)^2 + A_3 \left(\frac{x}{t}\right)^3 \qquad (2\text{-}1)$$

where x is the coordinate distance into the wall

t = wall thickness

σ = stress perpendicular to the plane of the crack

A_i = coefficients of the polynomial fit

The embedded flaw charts were constructed for a wide range of flaw sizes and shapes. The stress intensity factor calculation for embedded flaws was taken from work by Shah and Kobayashi [6], which is applicable to an embedded flaw in an infinite medium, subjected to an arbitrary stress profile. This expression has been shown to be applicable to embedded flaws in a pressure vessel in a paper by Lee and Bamford [7].

2.3 FRACTURE TOUGHNESS

The other key element in the determination of critical flaw sizes is the fracture toughness of the material. The fracture toughness has been taken directly from the reference curves of Appendix A, Section XI. In the transition temperature region, these curves can be represented by the following equations:

$$K_{Ic} = 33.2 + 2.806 \exp. [0.02 (T-RT_{NDT} + 100°F)] \quad (2\text{-}4)$$

$$K_{Ia} = 26.8 + 1.233 \exp. [0.0145 (T-RT_{NDT} + 160°F)] \quad (2\text{-}5)$$

where K_{Ic} and K_{Ia} are in ksi$\sqrt{\text{in}}$.

The upper shelf temperature regime requires utilization of a shelf toughness which is not specified in the ASME Code. A value of 200 ksi$\sqrt{\text{in}}$ has been used here. This value is consistent with general practice in such evaluations, as shown for example in reference [8], which provides the background and technical basis of Appendix A of Section XI.

The other key element in the determination of the fracture toughness is the value of RT_{NDT}, which is a parameter determined from Charpy V-notch and

drop-weight tests. The weld seams and plates used in the construction of the Waterford Unit 3 reactor vessel outlet nozzle regions are identified in Table 2-5.

The fracture properties of the outlet nozzle to vessel weld region were taken from the ASME Code Section XI Appendix A. The reference toughness curves are adjusted for the value of RT_{NDT} of the material. Table 2-5 contains the values for the nozzle forgings and upper shell material, taken from the Final Safety Analysis Report [9]. Test results were unavailable for the nozzle to shell weld material, but it was made with Linde 0091 weld material. A range of tests of over 80 combinations of weld wire and Linde 0091 flux, as summarized in table 6-4 of reference 4, shows the highest RT_{NDT} value to be -10°F. This information, along with the guidelines provided in Regulatory Guide 1.99 Revision 2 [10] leads to the conclusion that RT_{NDT} of the weld metal will be no higher than 0°F.

2.4 IRRADIATION EFFECTS

The level of irradiation damage at the outlet nozzle to shell weld of the Waterford Unit 3 reactor vessel is at least three orders of magnitude lower than at the core midplane. The end of life fluence for the vessel inner surface was calculated based on operation at rated power for 32 EFPY and assuming that exposure for all cycles is the same. The end of life fast neutron fluence at the vessel inner surface of the core midplane is 3.31 E19 N/SQCM based on this calculation [3]. Reducing this fluence appropriately for the outlet nozzle centerline (199.25 inches above the core midplane) the applicable fluence is at least three orders of magnitude lower. The indications closest to the core were designated 1BB, at 31.8 degrees from the top of the nozzle, and 2CC at 300.9 degrees from the nozzle top. These locations are approximately 15 inches above the centerline of the nozzle and this additional height results in a further reduction in fluence by nearly a factor of 10.

The fluences quoted above have been taken directly from figure 8 of reference [11], which is reproduced here as figure 2-1. The actual distance from the

core mid plane to the centerline of the nozzle is 199.25 inches, as shown in figure 2-2, and the indication at the lowest elevation is an additional 14.8 inches above this, for a total distance of 214.4 inches. This high elevation results in an applicable fluence of at least four orders of magnitude lower than the peak fluence at the core mid plane.

This value would be further reduced by the fact that the indications are embedded, and near the outside surface. Clearly at these fluences irradiation damage is negligible.

2.5 ALLOWABLE FLAW SIZE DETERMINATION

The applied stress intensity factor (K_I) and the material fracture toughness values (K_{Ia} and K_{Ic}) can be used to determine the allowable flaw size values used to construct the handbook charts. For normal, upset and test conditions, the allowable flaw size is determined as the depth at which the applied stress intensity factor K_I exceeds the arrest fracture toughness K_{Ia} divided by $\sqrt{10}$. This is the margin required by IWB 3612. This determination is shown as an example in figure 2-3, along with the stress distribution for the governing transient, the 3105 psi hydrotest.

For emergency and faulted conditions the allowable flaw size is obtained from the intersection of the applied stress intensity factor (K_I) curve with the static fracture toughness (K_{Ic}) divided by $\sqrt{2}$, the appropriate margin. This determination is shown as an example in figure 2-4, along with the stress distribution for the worst case faulted condition, as discussed in section 2.1.2. By comparing these two figures, it is clear that the normal upset and test conditions produce a smaller allowable flaw size, so the detailed development of the chart discussed in section 4 of the report proceeds on this basis.

2.6 STRESS CORROSION CRACKING SUSCEPTIBILITY

In evaluating flaws, all mechanisms of subcritical crack growth must be evaluated to ensure that proper safety margins are maintained during service. Stress corrosion cracking has been observed to occur in stainless steel in

operating BWR piping systems; the discussion presented here is the technical basis for not considering this mechanism in the present analysis.

For all pressurized water reactors, there is no history of stress corrosion cracking failure in the reactor coolant system loop. For stress corrosion cracking (SCC) to occur, the following three conditions must exist simultaneously: high tensile stresses, a susceptible material, and a corrosive environment. Since some residual stresses and some degree of material susceptibility exist in any stainless steel material, the potential for stress corrosion is minimized by proper selection of materials immune to SCC as well as preventing the occurrence of a corrosive environment. The material specifications consider compatibility with the system's operating environment (both internal and external) as well as other materials in the system, applicable ASME Code rules, fracture toughness, welding, fabrication, and processing.

The environments known to increase the susceptibility of austenitic stainless steel to stress corrosion are oxygen, fluorides, chlorides, hydroxides, hydrogen peroxide, and reduced forms of sulfur (e.g., sulfides, sulfites, and thionates). Strict cleaning standards prior to operation and careful control of water chemistry during plant operation are used to prevent the occurrence of a corrosive environment. Prior to being put into service, the piping is cleaned internally and externally. During flushes and preoperational testing, water chemistry is controlled in accordance with written specifications. External cleaning for Class 1 stainless steel piping includes patch tests to monitor and control chloride and fluoride levels. For preoperational flushes, influent water chemistry is controlled. Requirements on chlorides, fluorides, conductivity, and pH are included in the water chemistry specification.

During plant operation, the reactor coolant system (RCS) water chemistry is monitored and maintained within very specific limits. Contaminant concentrations are kept below the thresholds known to be conducive to stress corrosion cracking with the major water chemistry control standards being included in the plant operating procedures as a condition for plant operation. For example, during normal power operation, oxygen concentration in the RCS is

expected to be less than 0.005 ppm by controlling charging flow chemistry and maintaining hydrogen in the reactor coolant at specified concentrations. Halogen concentrations are also stringently controlled by maintaining concentrations of chlorides and fluorides within the specified limits. This is assured by controlling charging flow chemistry and specifying proper wetted surface materials.

TABLE 2-1
REACTOR TRANSIENTS - WATERFORD UNIT 3

TRANSIENT	OCCURRENCE (CYCLES)	OPERATING CONDITION SERVICE LIMITS
Normal, Upset and Test Conditions		
Heatup and Cooldown	500	Normal
Loading and Unloading	15,000	Normal
Transient Group 1		
10% step load increase		
10% step load decrease	1,000,000	Normal
Normal plant variations		
Transient Group 2		
Reactor Trip		
Loss of Flow	480	Upset
Loss of Load		
Leak Test	200	Test
Hydrostatic Test	10	Test
Operating Basis Earthquake	200	Upset
Emergency and Faulted Conditions		
Steam-line Breaks		
0.1-m^2 main steam-line break upstream of MSIVs		
(1) From HZP		
(2) From full power		
(3) From HZP with two operating reactor coolant pumps		
Double-ended main steam-line break upstream of MSIVs		
(4) From HZP with continued EFW flow to broken SG*		
(5) From HZP with two stuck-open MSIVs		
Small steam-line break downstream of MSIVs		
(6) From full power		
(7) From full power with one stuck-open MSIV		
Runaway Feedwater		
(8) Runaway MFW to two SGs from full power		
(9) Runaway MFW to one SG from full power		
(10) Runaway EFW to two SGs from full power		
Small-Break Loss-of-Coolant Accidents		
(11) 0.002-m^2 hot-leg break from full power		

Notes
HZP = hot zero power
MFW = main feedwater
EFW = emergency feedwater
MSIV = main steam isolation valve
SG = steam generator
*Not applicable to Waterford plant but included in generic study of [5]

TABLE 2-2. LTOP EVENT TREE FOR BEST ESTIMATE CALCULATION

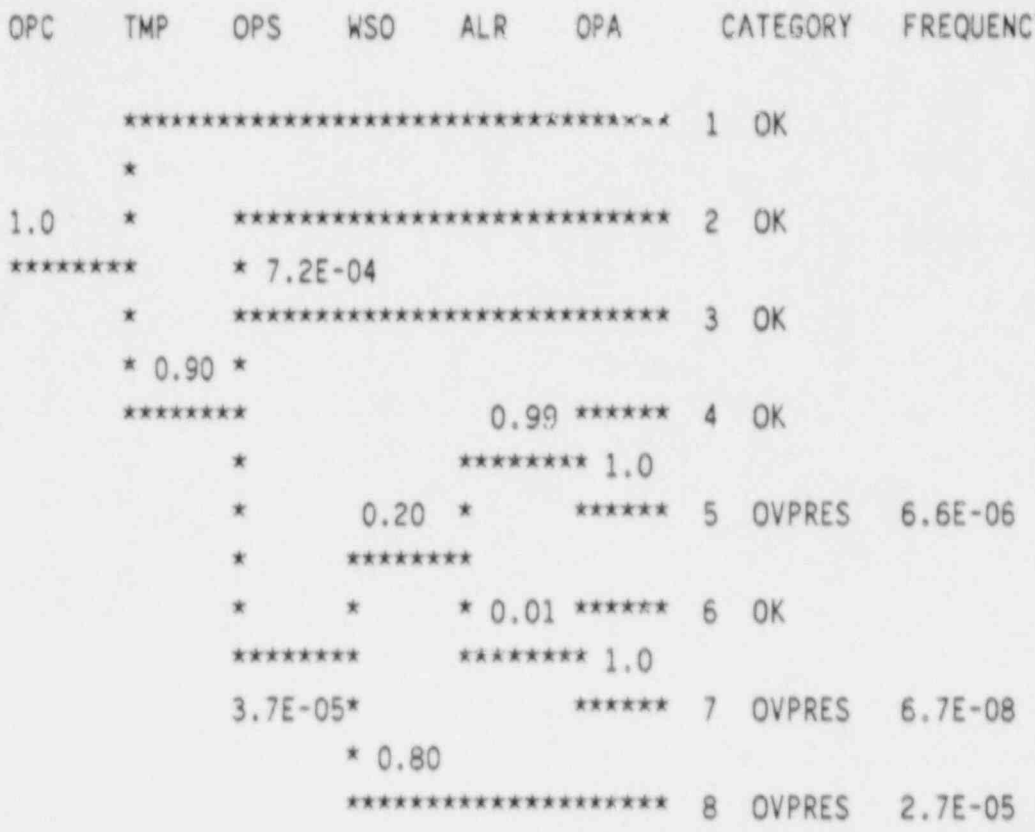

CATEGORY DESCRIPTION

OK OVERPRESSURE EVENT IS MITIGATED

OVPRES OVERPRESSURE SPIKE OCCURS

TOTAL FREQUENCY OF SIGNIFICANT OVERPRESSURE EVENT IS

3.4E-05 / CALENDAR YEAR

TABLE 2-3. LTOP EVENT TREE FOR CONSERVATIVE CALCULATION

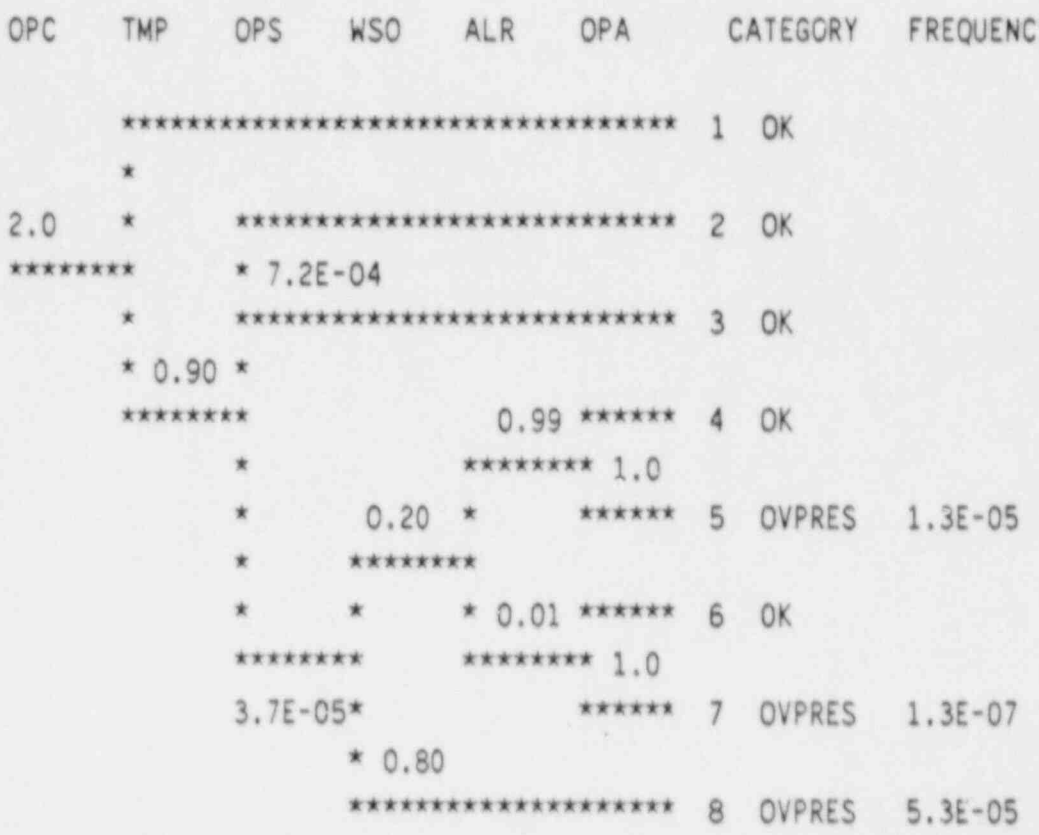

CATEGORY DESCRIPTION

OK OVERPRESSURE EVENT IS MITIGATED

OVPRES OVERPRESSURE SPIKE OCCURS

TOTAL FREQUENCY OF SIGNIFICANT OVERPRESSURE EVENT IS

6.6E-05 / CALENDAR YEAR

EVENT FREQUENCY RANGE (per reactor-year)	PLANT CONDITIONS CATEGORIES	OTHER CATEGORIZATION SCHEMES					
		NRC			ANS		
		10 CFR	RG 1.48 ASME Code*	RG 1.70 Rev. 2	51.1 (N18.2)	52.1 (N212)	53.1 (N213)
Planned Operations	PC-1	Normal	Normal	Normal	Condition I	Normal PPC	Plant Condition A
10^{-1}	PC-2	Anticipated Operational Occurrences	Upset	Moderate Frequency	Condition II	Frequent PPC	Plant Condition B
10^{-2}	PC-3			Infrequent Incidents	Condition III		
10^{-3}	PC-4		Emergency			Infrequent PPC	Plant Condition C
10^{-4}		Accidents		Limiting Faults	Condition IV		
10^{-5}	PC-5		Faulted			Limiting PPC	Plant Condition D
10^{-6}							
	Not Considered						

*This terminology has been eliminated from 1977 version of the ASME Code.

TABLE 2-4

EVENT CATEGORIZATION RELATIVE TO EVENT FREQUENCY

TABLE 2-5

MATERIAL PROPERTIES OF REACTOR VESSEL OUTLET NOZZLE TO SHELL WELD REGION

WATERFORD UNIT 3

Location	Material Type	Drop Wt. NDTT (°F)	RT_{NDT} (initial)
Upper Shell			
M1002-1	plate	-40°F	-8°F
M1002-2	plate	-20	-20
M1002-3	plate	-40	-40
Nozzle-to-Shell	weld*		
01-021		N/A	0°F
01-024		N/A	0°F
Outlet Nozzles			
M1011-2	forging	-20	-20
M1011-1	forging	0	0

*Note: all welds made with Linde 0091 flux.

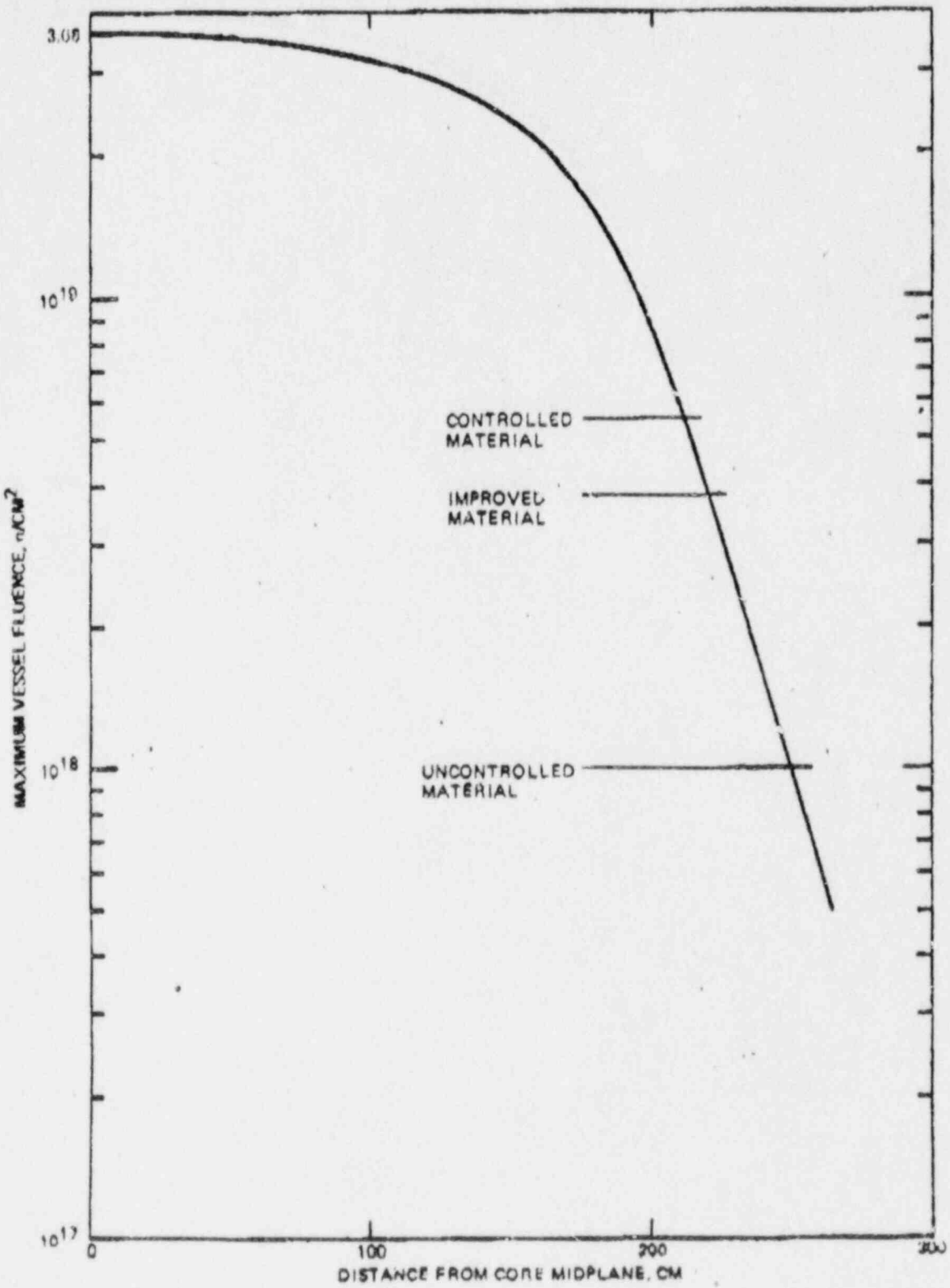

Figure 2-1 EOL Peak Fast Neutron Exposure as a Function of Axial Location in the Waterford Unit 3 Pressure Vessel [11]

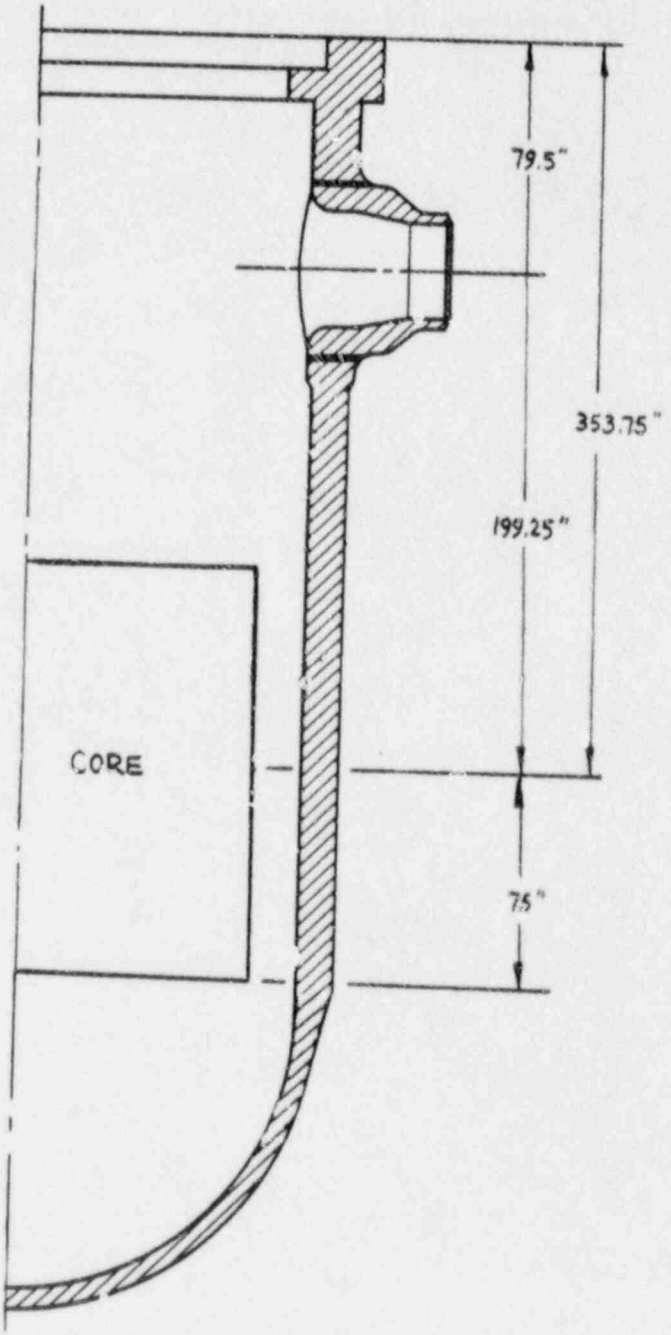

Figure 2-2 Identification and Location of Reactor Vessel Material for the Waterford Unit No. 3 Reactor Vessel

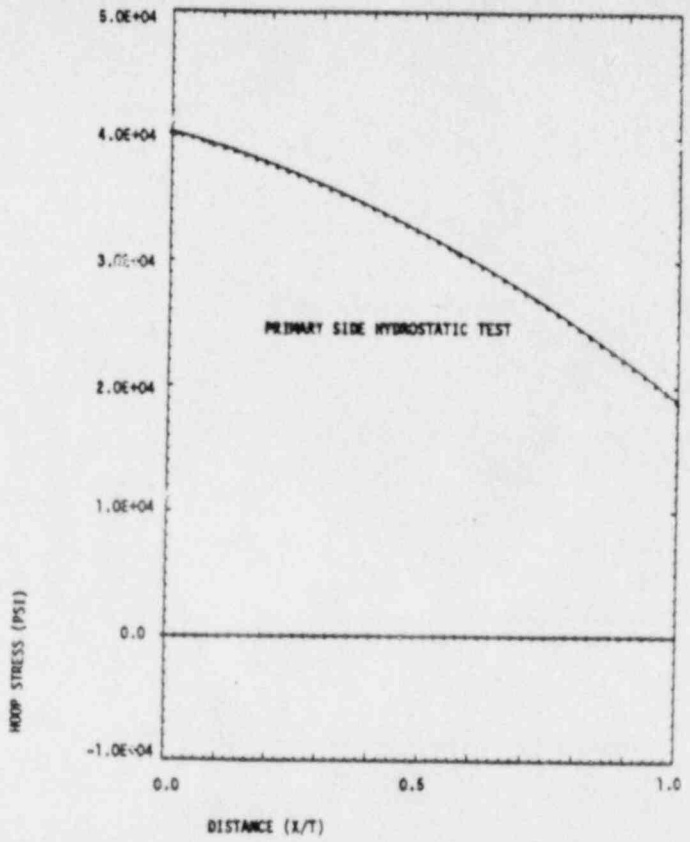

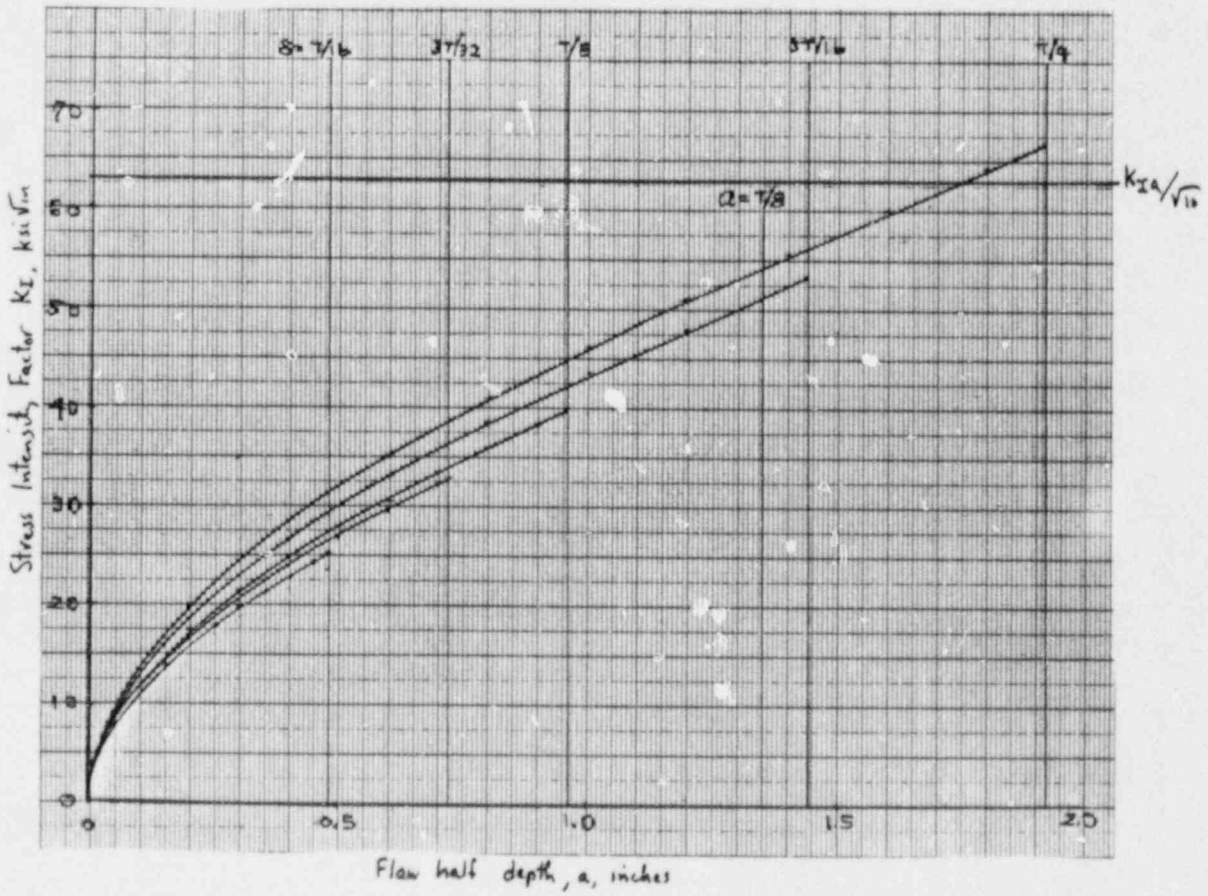

Figure 2-3 Stress distribution and Stress Intensity Factor Results for the Governing Normal, Upset, and Test Condition, the Primary Side Hydrotest at 3105 psi

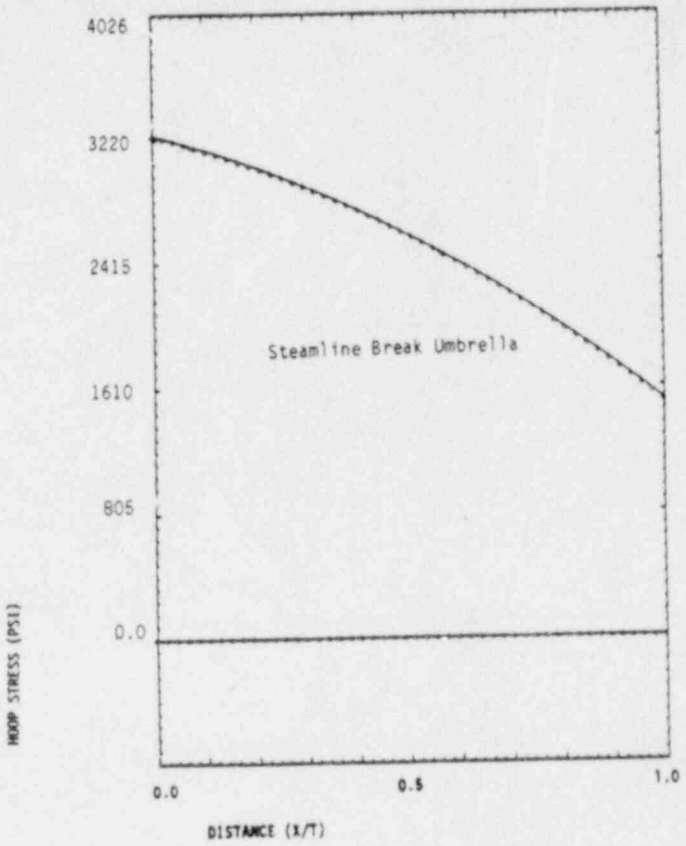

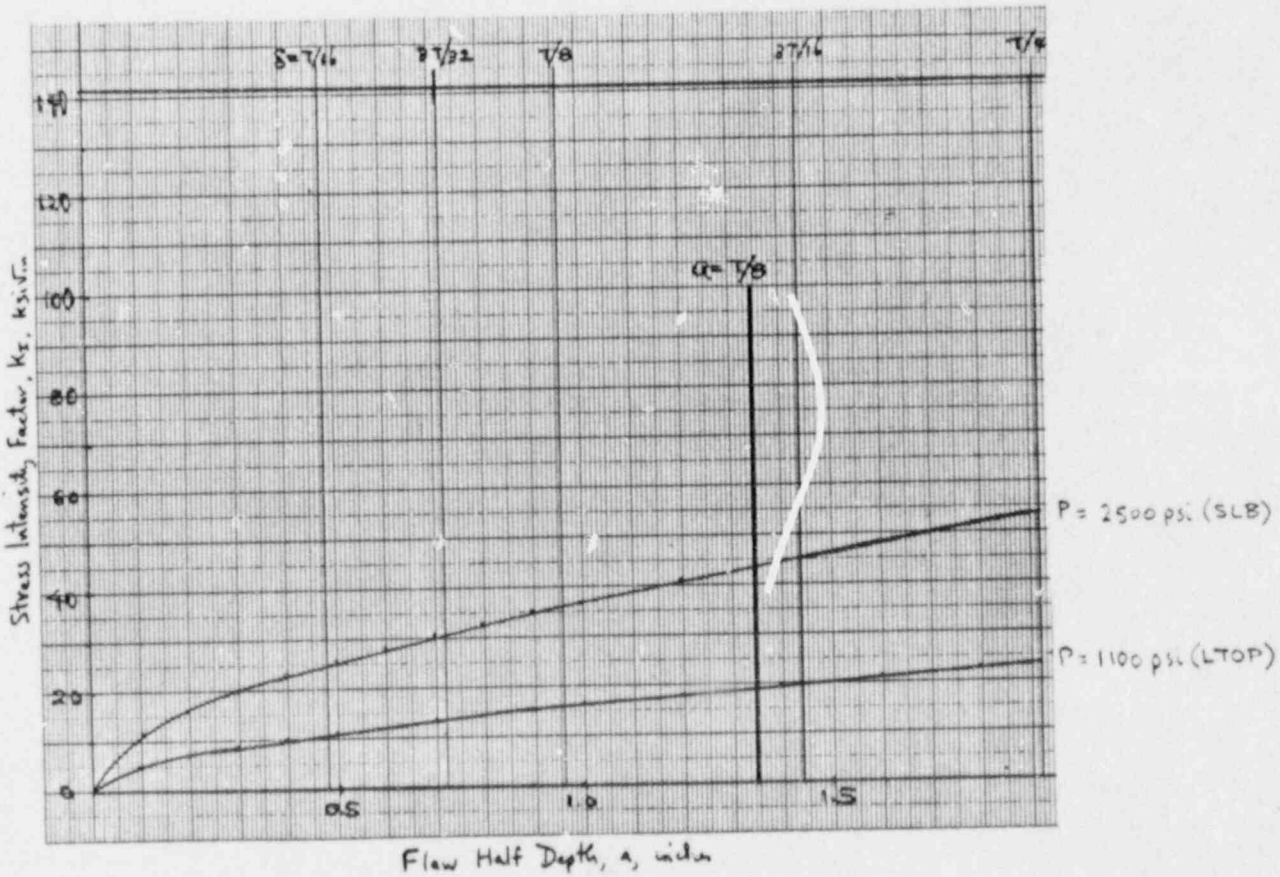

Figure 2-4 Stress Distribution and Stress Intensity Factor Results for the Governing Emergency and Faulted Conditions (steamline break umbrella at 2500 psi) and the LTOP Event

SECTION 3
FATIGUE CRACK GROWTH

In applying code acceptance criteria introduced in section 1 of this report, the final flaw size a_f is defined as the flaw size to which the detected flaw is calculated to grow at the end of the specified service period. In the handbook charts, ten-, twenty-, and thirty-year service periods are assumed.

These crack growth calculations have been carried out for the reactor vessel outlet nozzle to shell weld region of the Waterford Unit 3 reactor vessel, for which evaluation charts have been constructed. The crack growth calculations reported here are rather extensive, because a range of flaw shapes have been considered, to encompass the range of flaw shapes which could be encountered in service. This section will examine the calculations, and provide the methodology used as well as the assumptions.

3.1 ANALYSIS METHODOLOGY

The fatigue crack growth analysis procedure involves postulating an initial flaw at a specific region and predicting the growth of that flaw due to an imposed series of loading transients. The input required for a fatigue crack growth analysis is basically the information necessary to calculate the parameter ΔK_I which depends on crack and structure geometry and the range of applied stresses in the area where the crack exists. Once ΔK_I is calculated, the growth due to that particular stress cycle can be calculated by equations given in section 3.3 and figure 3-1. This increment of growth is then added to the original crack size, and the analysis proceeds to the next transient. The procedure is continued in this manner until all the transients known to occur in the period of evaluation have been analyzed.

The transients considered in the analysis are all the design transients as shown in section 2, table 2-1. These transients are spread equally over the design lifetime of the vessel, with the exception that the preoperational

tests are considered first. Faulted conditions are not considered in the crack growth analysis because their frequency of occurrence is too low to affect fatigue crack growth.

Crack growth calculations were carried out for a range of embedded flaw depths, with flaw length equal to five times its width. For all cases the flaw was assumed to maintain a constant shape as it grew. Calculations for other flaw shapes were unnecessary because the selected types conservatively model the crack growth of the flaws of interest for construction of the charts.

3.2 STRESS INTENSITY FACTOR EXPRESSIONS

Stress intensity factors were calculated from methods available in the literature for each of the flaw types analyzed.

For embedded flaws, the stress intensity factor expression of Shah and Kobayashi [6] was used, as discussed earlier in section 2.2. The flaw shape was set with length equal to five times the width ($a/\ell = 0.10$), and the eccentricity (location within the vessel wall thickness) was varied, as shown in the table 3-2. This flaw shape was chosen to provide a worst case calculation of stress intensity factor for embedded flaws. The calculated crack growth was very small for this case as may be seen in the table, so no other shapes were considered necessary for analysis.

3.3 CRACK GROWTH RATE REFERENCE CURVES

The crack growth rate curves used in the analyses were taken directly from figure A4300-1 of Appendix A of Section XI of the ASME Code. The air environment curve was used for the embedded flaws analyzed here. Although only the air curve was used, both air and water curves will be described, for completeness.

The reference crack growth curves are shown in figure 3-1. The crack growth rate in a water environment is a function of both the applied stress intensity factor range, and the R ratio (K_{min}/K_{max}) for the transient.

For $R \leq 0.25$

$$(\Delta K_I \leq 19 \text{ ksi}\sqrt{\text{in}}) \frac{da}{dN} = (1.02 \times 10^{-6}) \Delta K_I^{5.95}$$

$$(\Delta K_I > 19 \text{ ksi}\sqrt{\text{in}}) \frac{da}{dN} = (1.01 \times 10^{-1}) \Delta K_I^{1.95}$$

where $\frac{da}{dN}$ = Crack Growth rate, micro-inches/cycle.

For $R \geq 0.65$

$$(\Delta K_I \leq 12 \text{ ksi}\sqrt{\text{in}}) \frac{da}{dN} = (1.20 \times 10^{-5}) \Delta K_I^{5.95}$$

$$(\Delta K_I > 12 \text{ ksi}\sqrt{\text{in}}) \frac{da}{dN} = (2.52 \times 10^{-1}) \Delta K_I^{1.95}$$

For R ratio between these two extremes, interpolation is recommended.

The crack growth rate reference curve for air environments is a single curve, with growth rate being only a function of applied ΔK. This reference curve is shown in figure 3-1, along with the curves for water environment. The air curve was used for the analysis presented in this report. The equation is:

$$\frac{da}{dN} = (0.0267 \times 10^{-3}) \Delta K_I^{3.726}$$

where, $\frac{da}{dN}$ = Crack growth rate, micro-inches/cycle

ΔK_I = stress intensity factor range, ksi$\sqrt{\text{in}}$

$= (K_{Imax} - K_{Imin})$

3.4 FATIGUE CRACK GROWTH RESULTS

The fatigue crack growth results upon which handbook charts were developed are summarized in table 3-1.

TABLE 3-1
FATIGUE CRACK GROWTH RESULTS - WATERFORD UNIT 3
REACTOR VESSEL OUTLET NOZZLE TO SHELL REGION -
EMBEDDED FLAWS NEAR OUTSIDE SURFACE

δ = T/16

INITIAL DEPTH	CRACK DEPTH AFTER YEAR 10	20	30	40
0.40	0.40050	0.40096	0.40141	0.40186
0.45	0.45062	0.45117	0.45172	0.45228
0.48	0.48069	0.48131	0.48192	0.48255

δ = 3T/32 = 1.008

INITIAL DEPTH	CRACK DEPTH AFTER YEAR 10	20	30	40
0.600	0.60124	0.60235	0.60345	0.60457
0.700	0.70160	0.70303	0.70446	0.70590
0.720	0.72167	0.72317	0.72467	0.72618

δ = T/8 = 1.344

INITIAL DEPTH	CRACK DEPTH AFTER YEAR 10	20	30	40
800	0.80243	0.80459	0.80675	0.80893
900	0.90293	0.90554	0.90815	0.91079
950	0.95319	0.95603	0.95888	0.96175
960	0.96324	0.96613	0.96902	0.97195

δ = 3T/16 = 2.016

INITIAL DEPTH	CRACK DEPTH AFTER YEAR 10	20	30	40
1.00	1.00501	1.00941	1.01382	1.01828
1.10	1.10582	1.11094	1.11607	1.12126
1.20	1.20666	1.21252	1.21839	1.22434
1.30	1.30751	1.31413	1.32077	1.32749
1.40	1.50925	1.51742	1.52561	1.53390

δ = T/4 = 2.688

INITIAL DEPTH	CRACK DEPTH AFTER YEAR 10	20	30	40
1.00	1.00696	1.01292	1.01891	1.02499
1.10	1.10811	1.11508	1.12208	1.12919
1.20	1.20931	1.21732	1.22537	1.23355
1.30	1.31054	1.31962	1.32876	1.33804
1.50	1.51307	1.52438	1.53576	1.54732

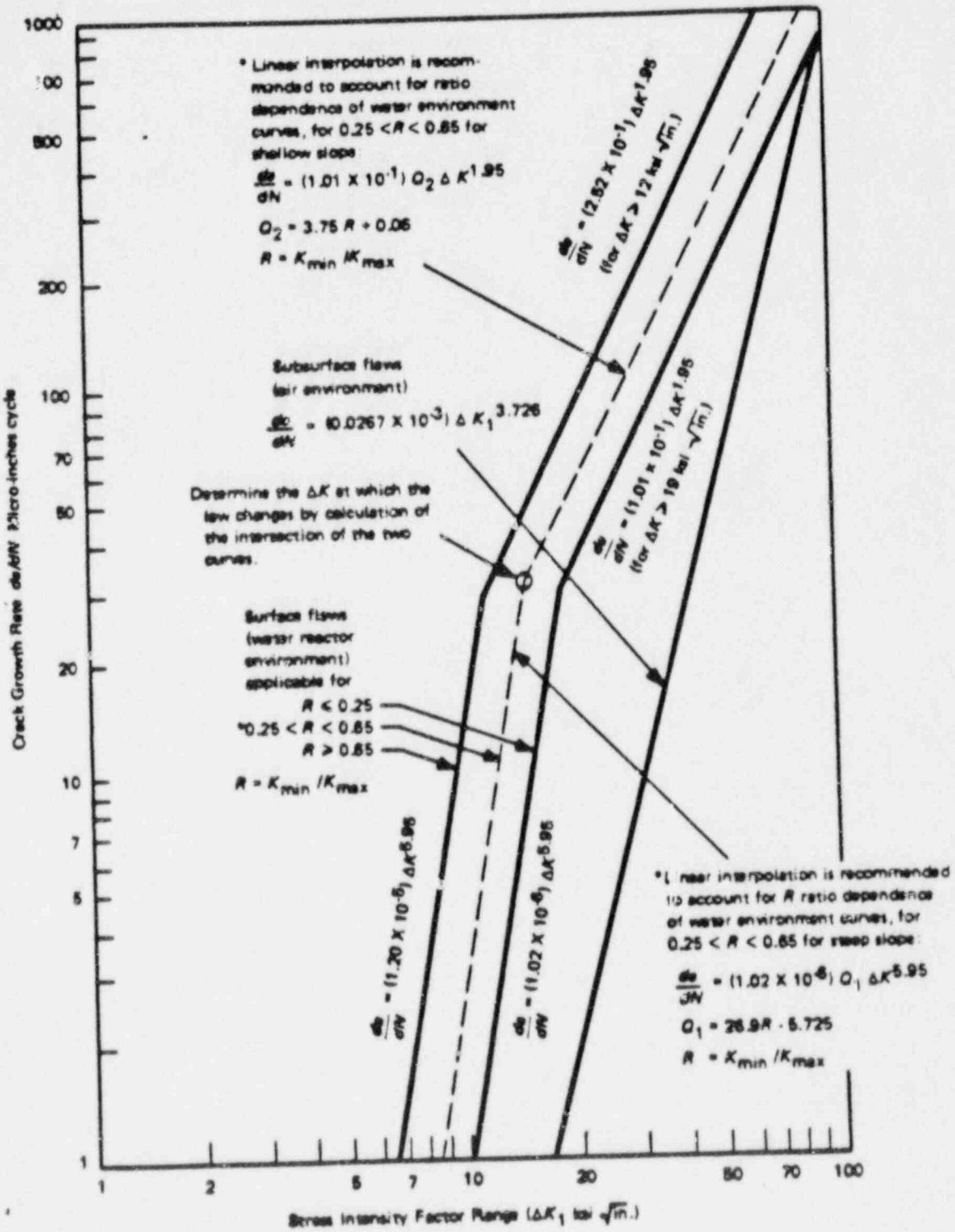

Figure 3-1. Reference Fatigue Crack Growth Curves for Carbon and Low Alloy Ferritic Steels

SECTION 4
EMBEDDED FLAW EVALUATION

4.1 SCOPE OF EVALUATION

Embedded flaw evaluation charts were developed for the outlet nozzle to shell region. This section describes the development of the embedded flaw charts for that region, and provides a detailed example, for indications near the outside surface. The construction of the charts follows the Section XI flaw evaluation methodology directly, as illustrated in figure 4-1.

4.2 EMBEDDED VS. SURFACE FLAWS

According to IWA-3300 of the ASME Code Section XI, a flaw is defined as embedded, as shown in figure 4-2, whenever,

$$S \geq 0.4\ a \qquad (4\text{-}1)$$

where

S - the minimum distance from the flaw edge to the nearest vessel wall surface

a - the embedded flaw depth, (defined as the semi-minor axis of the elliptical flaw.)

The parameter δ has been defined in this document to facilitate the use of the charts. δ is defined as the distance from the centerline of the flaw to the surface of the vessel. Therefore, $\delta = S + a$. Substituting into the proximity limit in equation 4-1 gives a limiting definition of δ as a function of a, for the proximity limit.

$$a = \delta - S \qquad (4\text{-}2)$$

$$\delta \geq 1.4\ a \qquad (4\text{-}3)$$

Therefore, the limit for a flaw to be considered embedded is $a_o = 0.714\ \delta$.

A flaw lying within the embedded flaw domain is to be evaluated by the embedded flaw evaluation charts generated in this section. On the other hand, a flaw lying beyond this domain should be evaluated as a surface flaw. The demarcation line between the two domains is shown graphically in figure 4-3.

4.3 CODE CRITERIA

As mentioned in section 1, the criteria used in most of the cases for embedded flaws are of IWB-3612 of Code Section XI. Namely,

$$K_I < \frac{K_{Ia}}{\sqrt{10}} \quad \text{For normal conditions (upset \& test conditions inclusive)} \quad (4\text{-}4)$$

$$K_I < \frac{K_{Ic}}{\sqrt{2}} \quad \text{For faulted conditions (emergency conditions inclusive)} \quad (4\text{-}5)$$

where

K_I = The maximum applied stress intensity factor for the flaw size a_f to which a detected flaw will grow, during the period of evaluation, which must be at least until the next inspection.

K_{Ia} = Fracture toughness based on crack arrest for the corresponding crack tip temperature.

K_{Ic} = Fracture toughness based on fracture initiation for the corresponding crack tip temperature.

The above two criteria must both be met. In this handbook only the most limiting results have been used as the basis of the flaw evaluation charts.

4.4 BASIC DATA

In view of the criteria based on stress intensity factor, three basic groups of data are needed for construction of embedded flaw evaluation charts. They are: a_f, driving force (K_I), and fracture toughness (K_{Ia} and K_{Ic}).

K_{Ic} and K_{Ia} are the initiation and arrest fracture toughness (respectively) of the vessel material at which the flaw is located. They can be calculated by formulas:

$$K_{Ic} = 33.2 + 2.806 \exp. [0.02(T-RT_{NDT} + 100°F)] \quad (4\text{-}6)$$

and

$$K_{Ia} = 26.8 + 1.233 \exp. [0.0145(T-RT_{NDT} + 160°F)] \quad (4\text{-}7)$$

K_I is the maximum stress intensity factor for the embedded flaw of interest. The methods used for determining the stress intensity factors for embedded flaws have been referenced in section 2.

Notice that both K_{Ic} and K_{Ia} are a function of crack tip temperature T, and the material property of RT_{NDT} at the tip of the flaw as discussed in section 2. The upper shelf fracture toughness of the vessel steel is assumed to be 200 ksi$\sqrt{in}$.

K_I used in the determination of the flaw evaluation charts is the maximum stress intensity factor of the embedded flaw under evaluation. It is important to note that the flaw size used for the calculation of K_I is not the flaw size detected by inservice inspection. Instead, it is the calculated flaw size which is projected to grow from the flaw size detected by inservice inspection after a specified period. That means that the embedded flaw size used for the calculation of K_I had to be determined by using fatigue crack growth results, as will be illustrated in this section.

4.5 FATIGUE CRACK GROWTH FOR EMBEDDED FLAWS

The environment of an embedded flaw is considered to be inert, or air. The crack growth rate for air environment is far smaller than that of the water environment, to which the surface flaw is conservatively considered to be exposed. Consequently, the fatigue crack growth for an embedded flaw is far smaller than that of an inside surface flaw (of the same size and under the same transient conditions). Numerically, the fatigue crack growth of an embedded flaw is so low that the difference between the initial flaw depth and its final crack depth is negligible, as demonstrated in table 3-2 for the nozzle to shell weld region.

4.6 TYPICAL EMBEDDED FLAW EVALUATION CHART

The details of the procedures for the construction of an embedded flaw evaluation chart are provided in the next section.

In this section, instructions for using an embedded flaw chart are provided by going through a typical chart, step by step. The example used here is for embedded flaws near the outside surface. This would help the users to become familiar with the characteristics of each part of the chart, and make it easier to apply. This example utilizes the surface/embedded flaw demarcation criteria of the code, as discussed earlier.

Following are the highlights of auxiliary curves used to construct the embedded flaw evaluation chart for the reactor vessel nozzle to shell weld region.

1. The abscissa of the chart in figures 4-4, 4-5, and 4-6 represents the flaw depth a, of the embedded flaw.

2. As defined by code requirements, embedded flaws with a depth less than $a_o = 0.714\ \delta$ should be considered as embedded flaws. Any embedded flaws beyond the domain of $a_o = 0.714\ \delta$, should be evaluated as a surface flaw.

3. A key parameter for evaluating an embedded flaw is δ, the distance between the centerline of the embedded flaw and the nearest surface of the wall.

   A range of δ between $\frac{1}{16}t$ and $\frac{1}{4}t$ has been considered in constructing figures 4-4, 4-5, and 4-6.

4. For each specific value of δ, such as $\frac{1}{8}t$, $\frac{3}{16}t$, $\frac{1}{4}t$, etc., a family of curves were plotted for a range of a/ℓ values ranging from .333 to .100. For any specific flaw depth a at the abscissa, a corresponding value K_I at the ordinate can be found in figures 4-4 through 4-6, for any distance to the surface, δ.

5. The range of a/ℓ values from 0.333 to 0.10 was chosen to encompass the range of flaws that might be detected. For the nozzle to shell weld region, fracture results are independent of the aspect ratio, as will be discussed further below.

6. In developing this specific chart, the code acceptance limit line of $K_{Ia}/\sqrt{10}$ as a function of flaw depth is shown in figures 4-4 through 4-6.

7. The intersection of the K_I curve with the code acceptance limit line is the maximum flaw size acceptable by code for the specific curve, in accordance with the $K_I \leq K_{Ia}/\sqrt{10}$ from IWB-3612.

8. In view of figures 4-4 through 4-6, it is seen that none of the curves intersect with the code acceptance limit line. That means that, up to a distance of $\delta = \frac{1}{4}$ t (= 2.688"), <u>all</u> embedded flaws are acceptable by the code criteria so long as their depth is within the domain of $a_o = 0.714\ \delta$, and their centerline falls within the outside half of the vessel.

9. The maximum acceptable flaw size can be found from the chart by determining the abscissa of the intersection points. Namely, for $\delta = 0.25$ t,

a/ℓ	Maximum Acceptable Flaw Depth a*(in.)
.100	1.34
.167	1.34 (= a_o = 1.34)
.333	1.34

10. The maximum acceptable embedded flaw size for $\delta = \frac{1}{4}t$ has been depicted in figure 4-3. This simple flaw evaluation chart, described in the following paragraph, is the type to be used for evaluation.

This embedded flaw evaluation chart, constructed for indications near the outside surface of the nozzle to shell region of the reactor vessel, is presented in figure 4-3.

4.7 PROCEDURE FOR THE CONSTRUCTION OF EMBEDDED FLAW EVALUATION CHARTS

This section shows how an embedded flaw evaluation chart was constructed for indications near the outer surface of the reactor vessel nozzle to shell weld region during the governing transient which is the hydrostatic test.

Step 1

Calculate K_I values for embedded flaws of various size near the outside surface, various aspect ratios, and at various distances underneath the surface. In total, 138 cases were analyzed by closed form stress intensity factor expressions. These 138 cases are listed in table 4-1.

Step 2

The K_I results of the 138 cases were plotted in figures 4-4 through 4-6.

---

* Maximum Acceptable Flaw Depth a is set at $\frac{1}{8}t$, based on engineering judgement, to limit the allowable through-wall penetration to 25 percent of the wall thickness.

Step 3

Determine the allowable flaw size, from $a_c/10$ or $K_I \leq K_{Ia}/\sqrt{10}$ criteria as determined by figures 4-4 through 4-6. Similar results could be obtained for the emergency/faulted conditions, but it can be seen from the surface flaw evaluation that they will not be governing so they have not been included here.

4.8 COMPARISON OF EMBEDDED FLAW CHARTS WITH ACCEPTANCE STANDARDS OF IWB-3500

The handbook charts for embedded flaws do not show the acceptance standards of Section XI, explicitly. Therefore, it is not clear from the charts themselves how much is gained from the analysis process over the standards tables contained in IWB-3500. Such a comparison cannot be made directly on the embedded flaw handbook charts, because the charts are applicable for a full range of sizes, shapes and locations. The purpose of this section is to provide such comparisons, and to discuss the results of those comparisons.

The handbook chart values have been compared with the acceptance standards tables in figure 4-7. In this figure the values from table IWB-3510-1 have been plotted as the base curve, and the limit curve for embedded flaws justified by analysis is shown as the other line. It can be seen that the range of embedded flaw shapes and depths justifiable by analysis is related to the flaw location within the wall. The deeper the indication, the more benefit is obtained from the analysis.

TABLE 4-1

EMBEDDED FLAW CASES ANALYZED FOR THE REACTOR VESSEL NOZZLE TO SHELL WELD REGION

DISTANCE OF FLAW TO SURFACE (δ in.)	EMBEDDED FLAW DEPTH (IN.) - T = 10.75 in.					
	A.R. 10:1		A.R. 6:1		A.R. 3:1	
T/16	0.05	0.10	0.05	0.10	0.05	0.10
	0.15	0.20	0.15	0.20	0.15	0.20
δ = 0.67188	0.25	0.30	0.25	0.30	0.25	0.30
	0.35	0.40	0.35	0.40	0.35	0.40
	0.45	0.47991	0.45	0.47991	0.45	0.47991
3T/32	0.10	0.20	0.10	0.20	0.10	0.20
	0.30	0.40	0.30	0.40	0.30	0.40
δ = 1.00781	0.50	0.60	0.50	0.60	0.50	0.60
	0.70	0.71987	0.70	0.71987	0.70	0.71987
T/8	0.10	0.20	0.10	0.20	0.10	0.20
	0.30	0.40	0.30	0.40	0.30	0.40
δ = 1.34375	0.50	0.60	0.50	0.60	0.50	0.60
	0.70	0.80	0.70	0.80	0.70	0.80
	0.90	0.95982	0.90	0.95982	0.90	0.95982
3T/16	0.20	0.40	0.20	0.40	0.20	0.40
	0.60	0.80	0.60	0.80	0.60	0.80
δ = 2.01563	1.00	1.20	1.00	1.20	1.00	1.20
	1.40	1.4397	1.40	1.4397	1.40	1.4397
T/4	0.20	0.40	0.20	0.40	0.20	0.40
	0.60	0.80	0.60	0.80	0.60	0.80
δ = 2.6875	1.00	1.20	1.00	1.20	1.00	1.20
	1.40	1.60	1.40	1.60	1.40	1.60
	1.80	1.91964	1.80	1.91964	1.80	1.91964

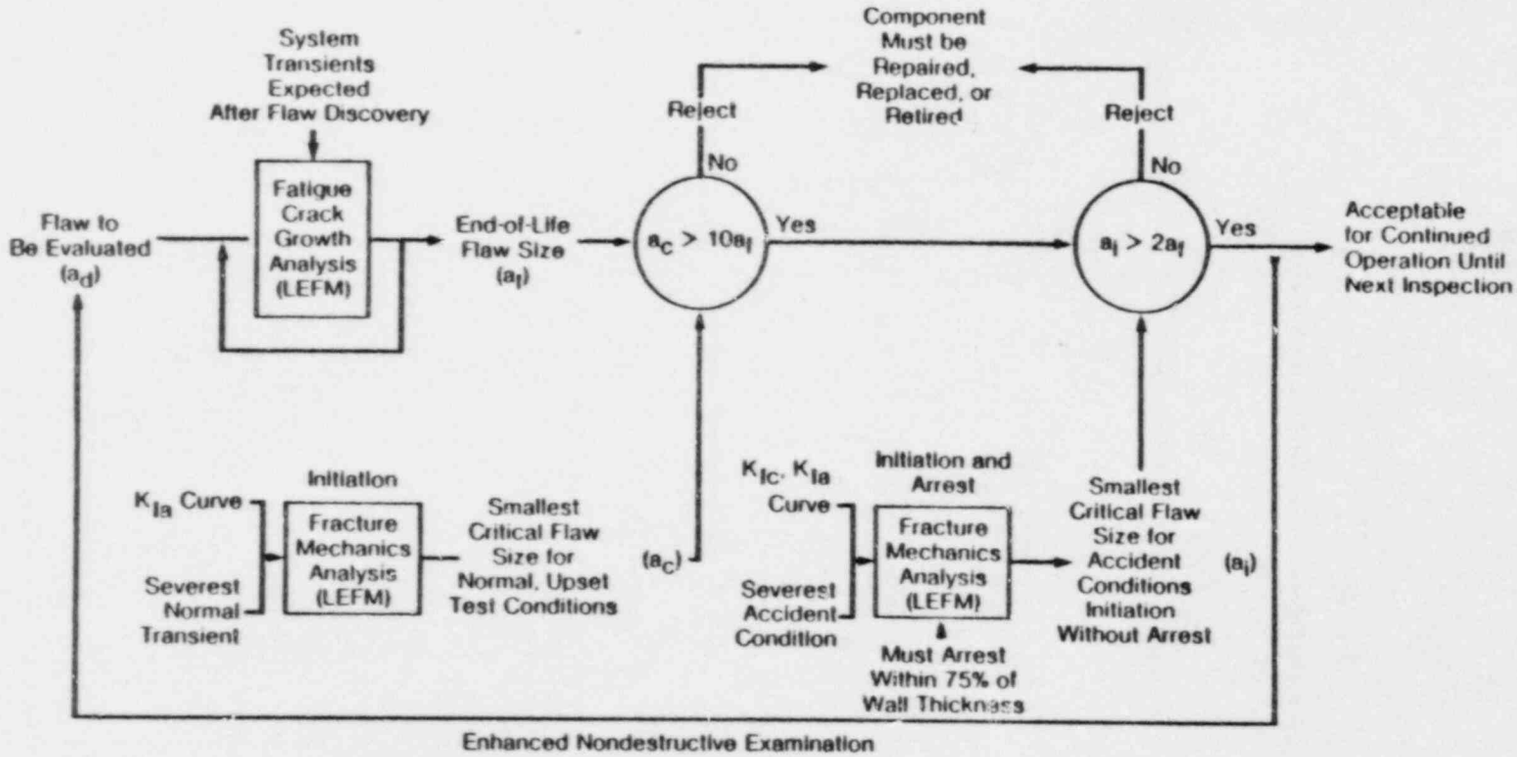

Figure 4-1 Schematic representation of Appendix A flaw evaluation process'

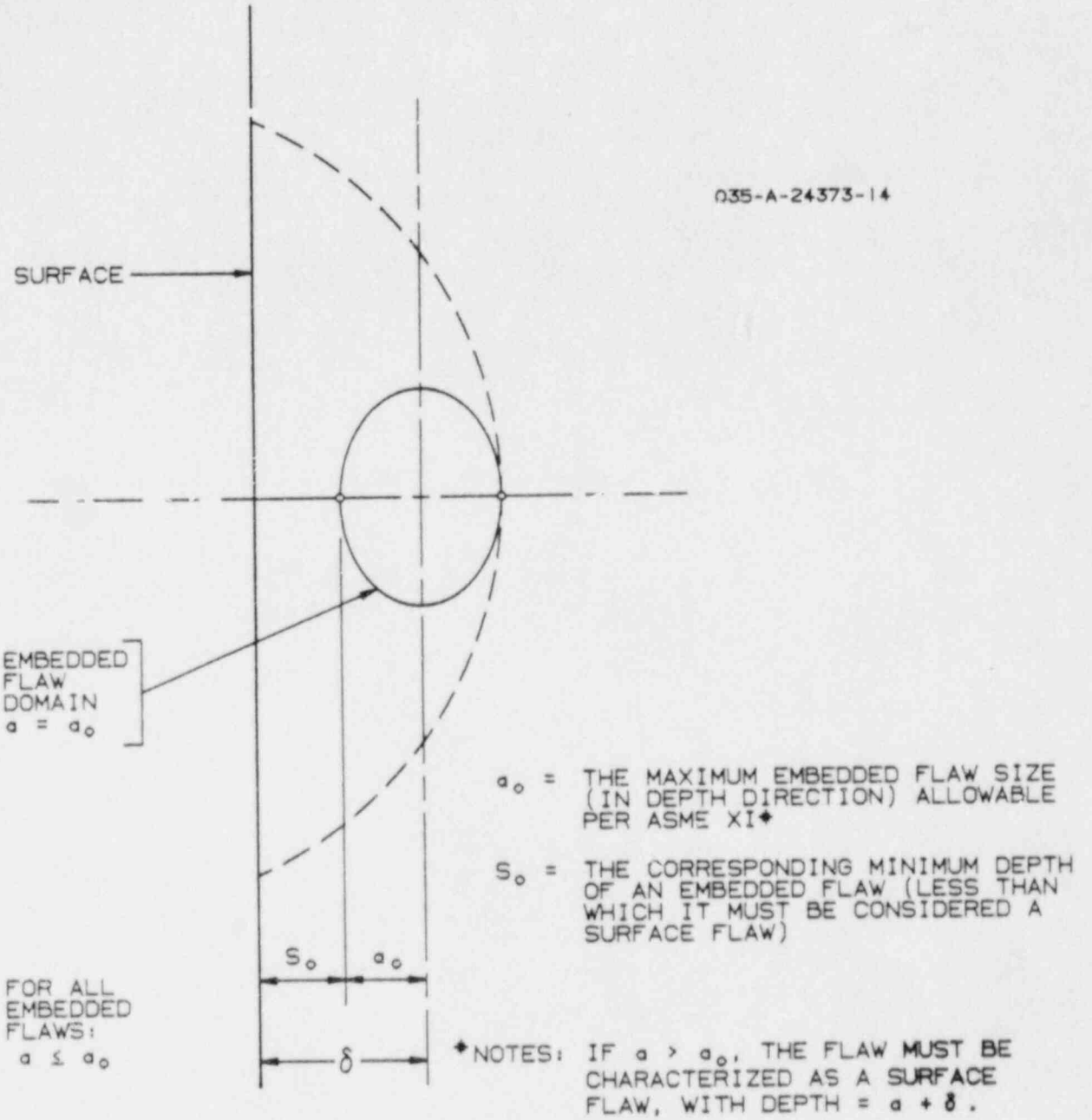

[a_o = 0.714δ FOR THE 1980 EDITION OF THE ASME CODE AND LATER EDITIONS]

Figure 4-2 Embedded vs. Surface Flaw

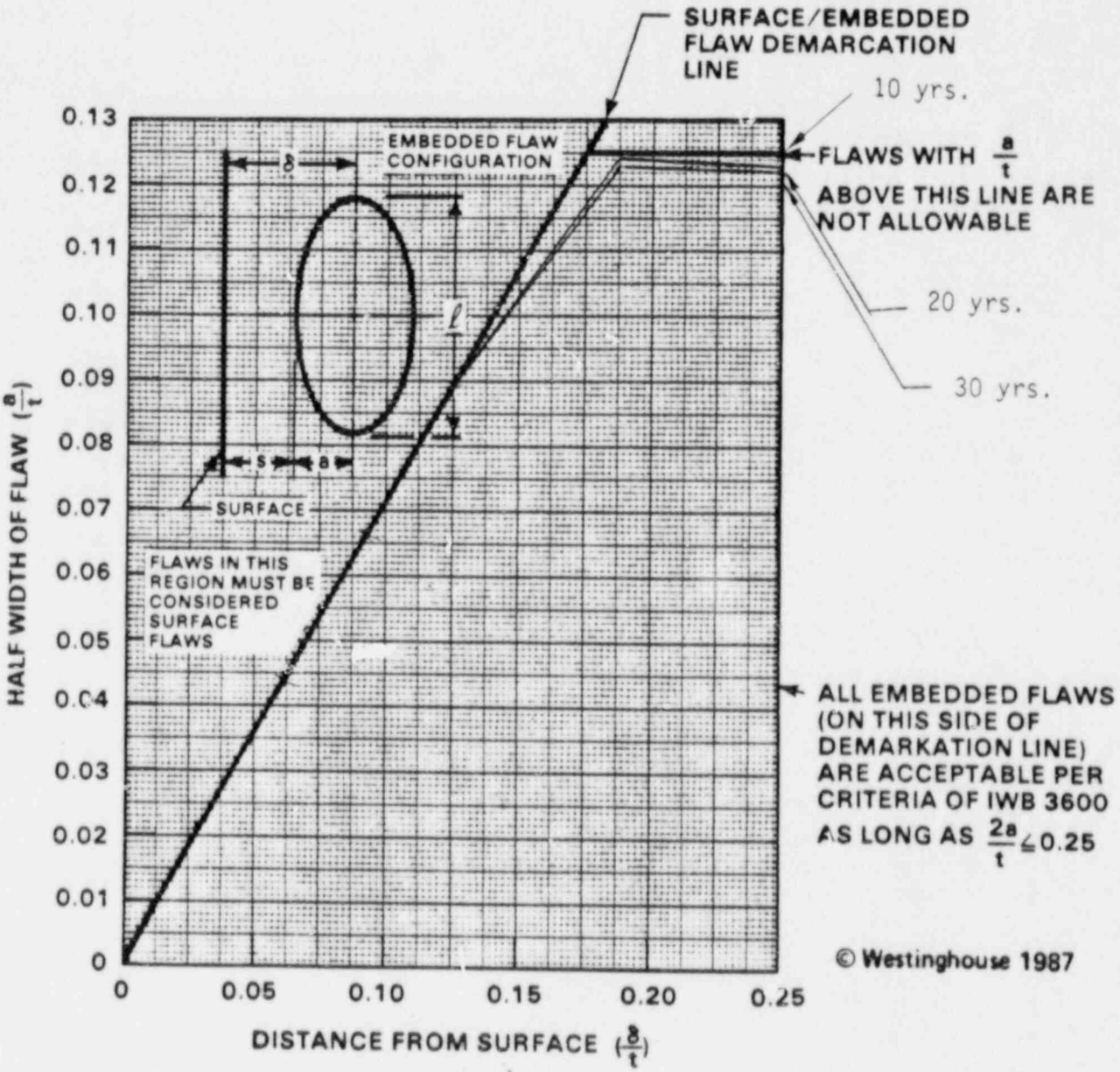

Figure 4-3 Embedded Flaw Evaluation Chart for Circumferential and Longitudinal Indications in the Reactor Vessel Nozzle to Shell Weld Region

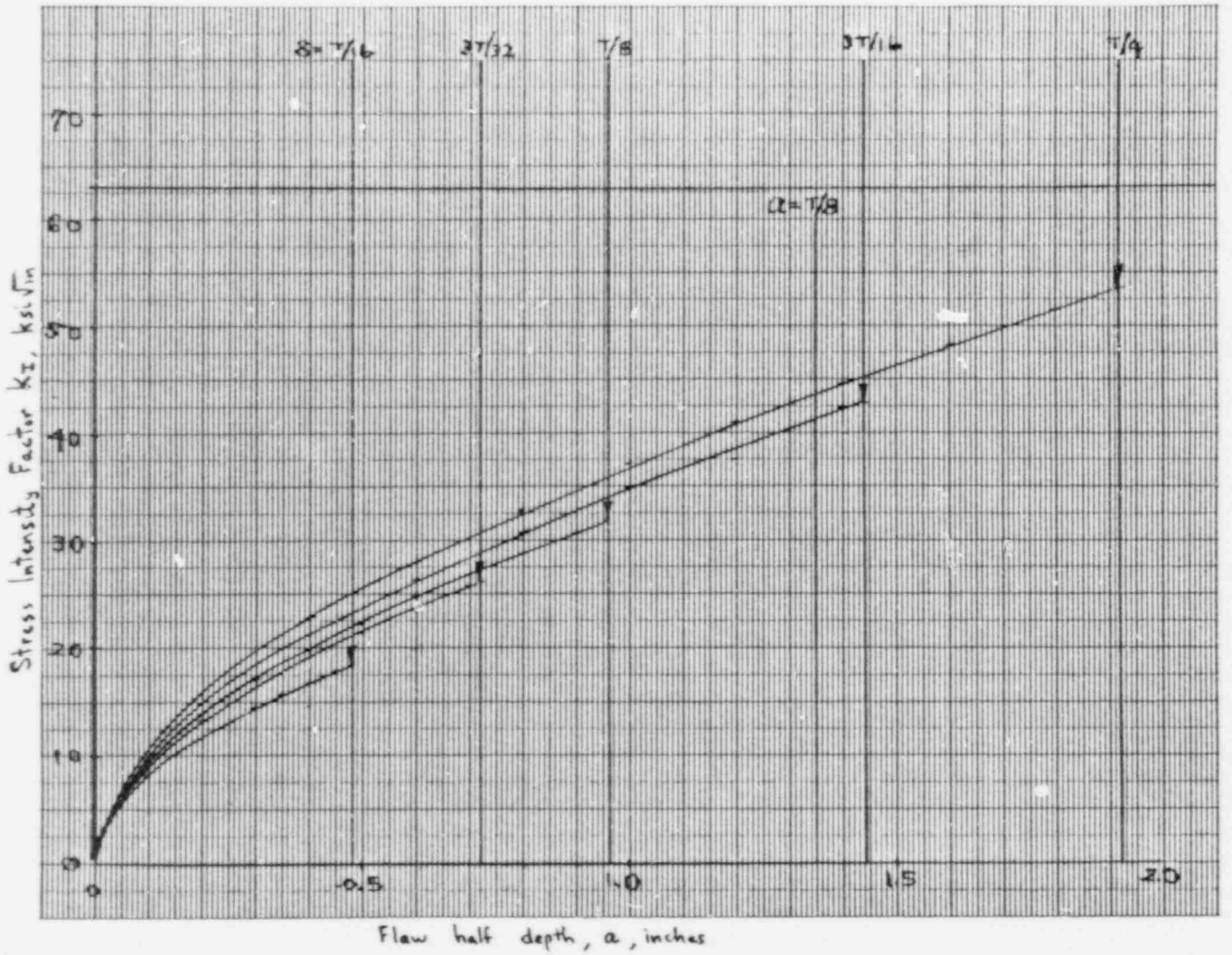

Figure 4-4 Stress Intensity Factor Plots for a/ℓ = 0.333 Used in Construction of Embedded Flaw Charts, Near the Outside Surface

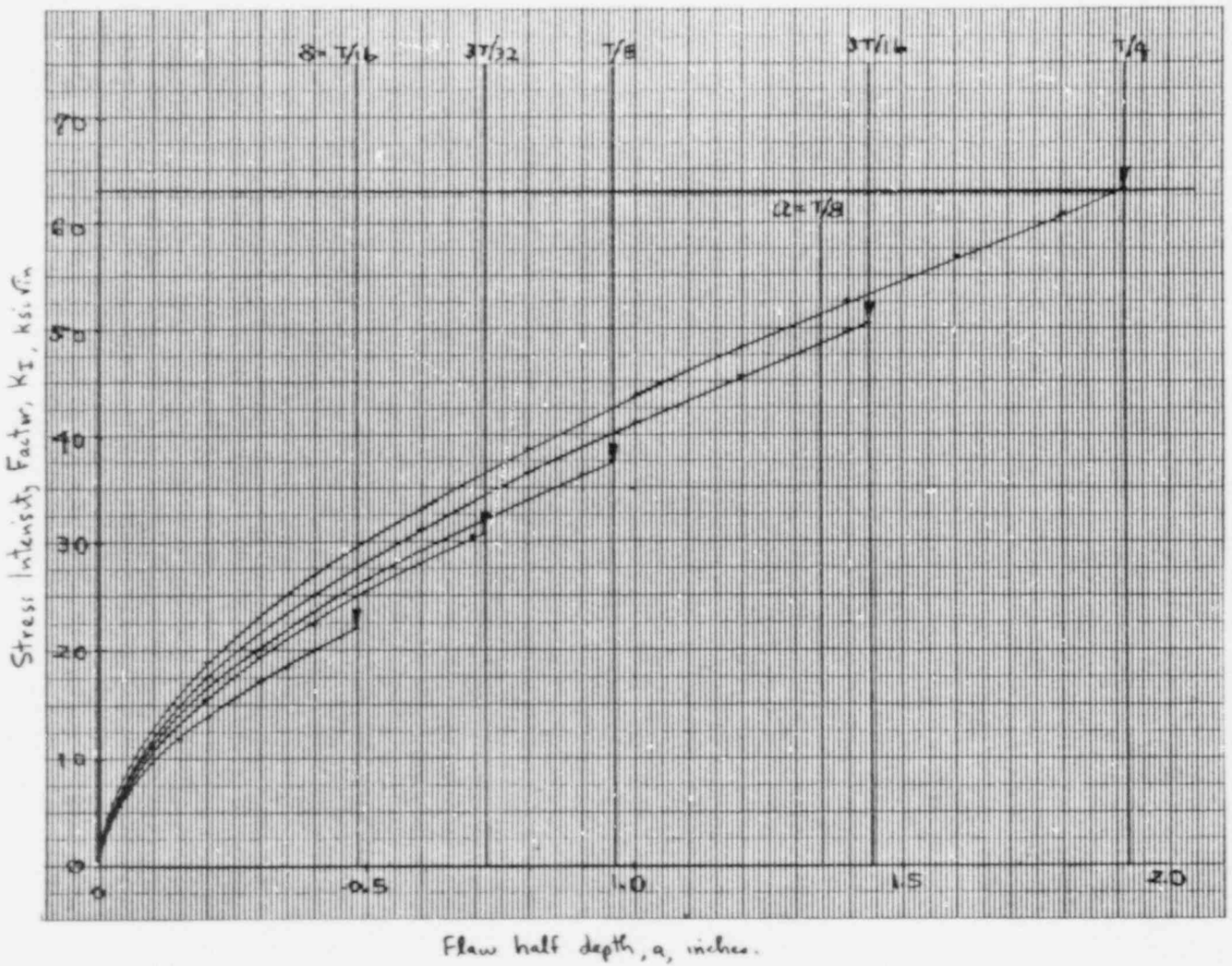

Figure 4-5 Stress Intensity Factor Plots for $a/\ell = 0.1667$ Used in Construction of Flaw Evaluation Charts, Near the Outside Surface

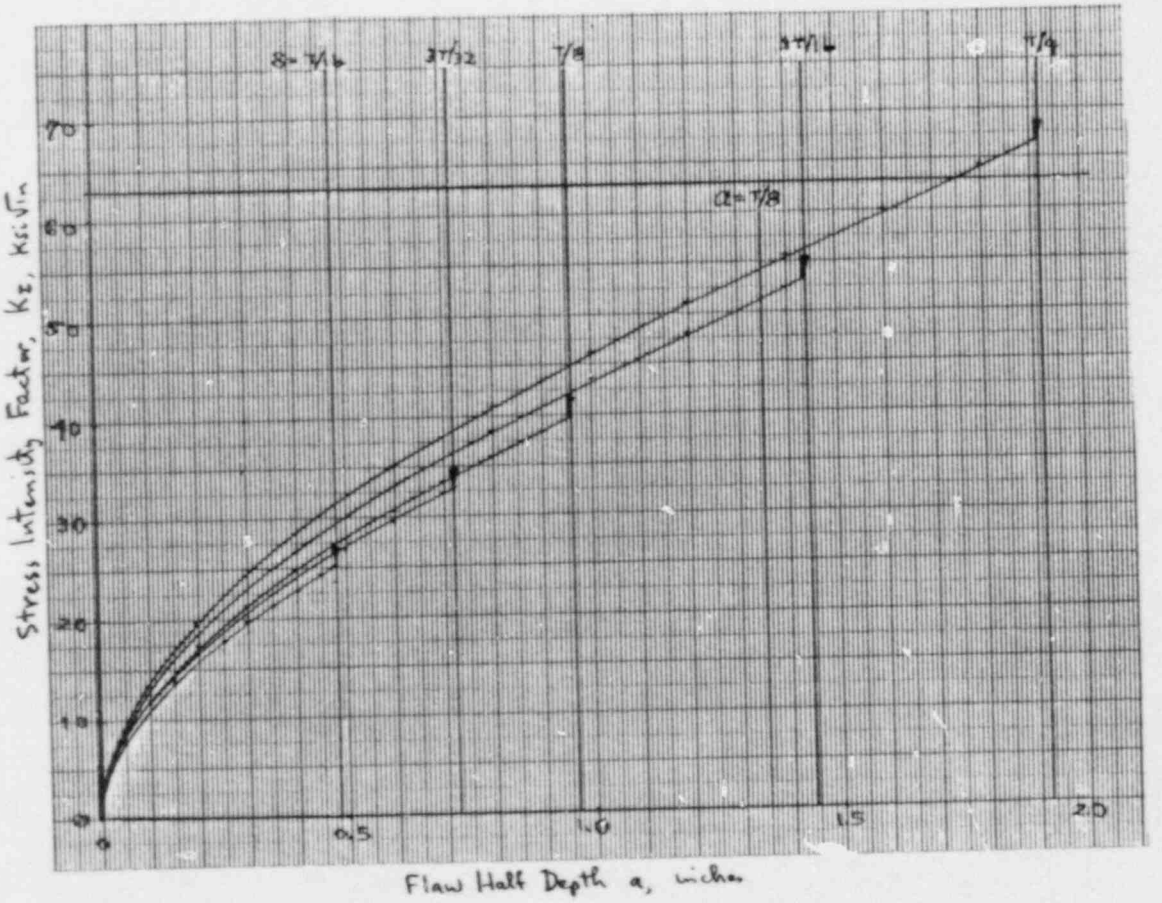

Figure 4-6 Stress Intensity Factor Plots for a/ℓ = 0.10 Used in Construction of Flaw Evaluation Charts, Near the Outside Surface

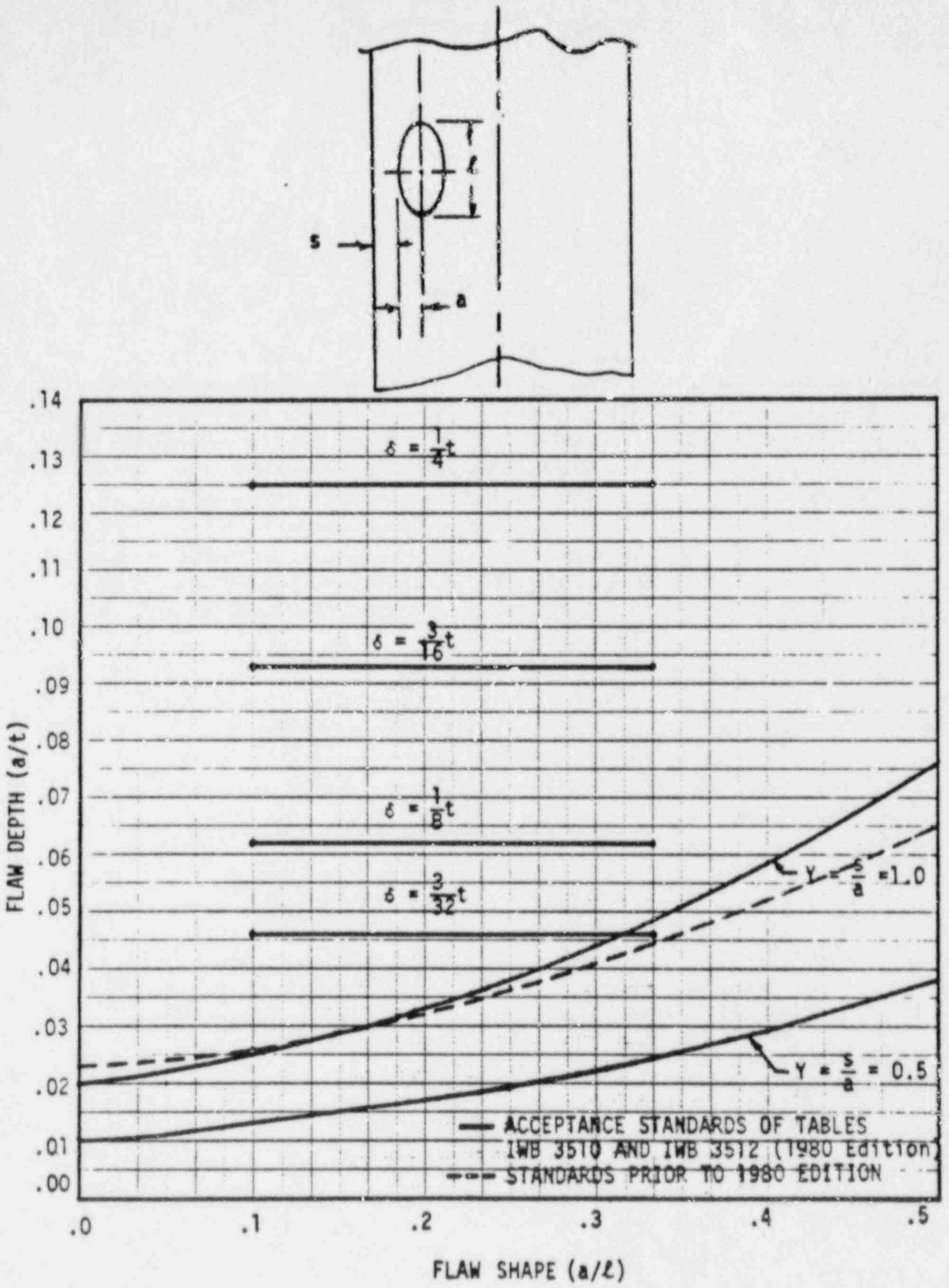

Figure 4-7 Acceptance Standards for Embedded Flaws, From Table IWB-3512-1

*Only Y = 1.0 curve applies to ASME Code prior to 1980 Edition.

SECTION 5
FLAW EVALUATION CHARTS-NOZZLE TO SHELL WELD REGION

5.1 EVALUATION PROCEDURE

The evaluation procedures contained in ASME Section XI are clearly specified in paragraph IWB-3600. Use of the evaluation charts herein follows these procedures directly, but the steps are greatly simplified.

Once the indication is discovered, it must be characterized as to its location, length (ℓ) and depth dimension (a for surface flaws, 2a for embedded flaws), including its distance from the surface (S) for embedded indications. This characterization is discussed in further detail in paragraph IWA-3000 of Section XI.

The following parameters must be calculated from the above dimensions to use the charts (see figure 1-2):

- Flaw Shape parameter, $\frac{a}{\ell}$
- Flaw depth parameter, $\frac{a}{t}$
- Surface proximity parameter (for embedded flaws only), $\frac{\delta}{t}$

where

t	=	wall thickness of region where indication is located (10.75 in.)
ℓ	=	length of indication
a	=	depth of surface flaw; or half depth of embedded flaw in the width direction
δ	=	distance from flaw centerline to surface (for embedded flaws only) ($\delta = s + a$)
s	=	smallest distance from edge of embedded flaw to surface

Once the above parameters have been determined and the determination made as to whether the indication is embedded or surface, then the two parameters may be plotted directly on the evaluation chart in figure 5-1. Its location on the chart determines its acceptability immediately.

5.2 IMPORTANT OBSERVATIONS ON THE HANDBOOK CHART

Although the use of the handbook charts is conceptually straight forward, experience in their development and use has led to a number of observations that will be helpful.

The evaluation chart for embedded flaws is shown in figure 5-1, and is applicable for both longitudinal and circumferential orientations throughout the wall thickness. The heavy diagonal line in the figure can be used directly to determine whether the indication should be characterized as an embedded flaw or whether it is sufficiently close to the surface that it must be considered as a surface flaw (by the rules of Section XI). If the flaw parameters produce a plotted point below the heavy diagonal line, it is acceptable by analysis. If it is <u>above</u> the line, it must be considered a surface flaw.

The standards for flaw acceptance without analysis cannot be shown in the embedded flaw charts because of their generality. Therefore, they have been plotted separately in figure 5-2.

A detailed examples of the use of the chart for embedded flaws is presented in the following section.

5.3 EMBEDDED FLAW EXAMPLE

Assume that a circumferential embedded flaw of 0.697 x 5.00", located within 0.824" from the surface, was detected. Determine whether this flaw should be considered as an embedded flaw.

$2a = 0.697"$

$S = 0.824"$

$\delta = S + a = 0.824 + 1/2\ (0.697) = 1.172"$

$t = 10.75"$

$\ell = 5.0"$

and,

$a = 1/2 \times 0.697"$

$= 0.348"$

Using figure 5-3:

$$\frac{a}{t} = \frac{0.348}{10.75} = 0.0324$$

$$\frac{\delta}{t} = \frac{1.172}{10.75} = 0.109$$

Since the plotted point (X) is below the diagonal demarcation line, the flaw must be considered embedded. Since it is below the a/t = .125 limit line, the indication is acceptable.

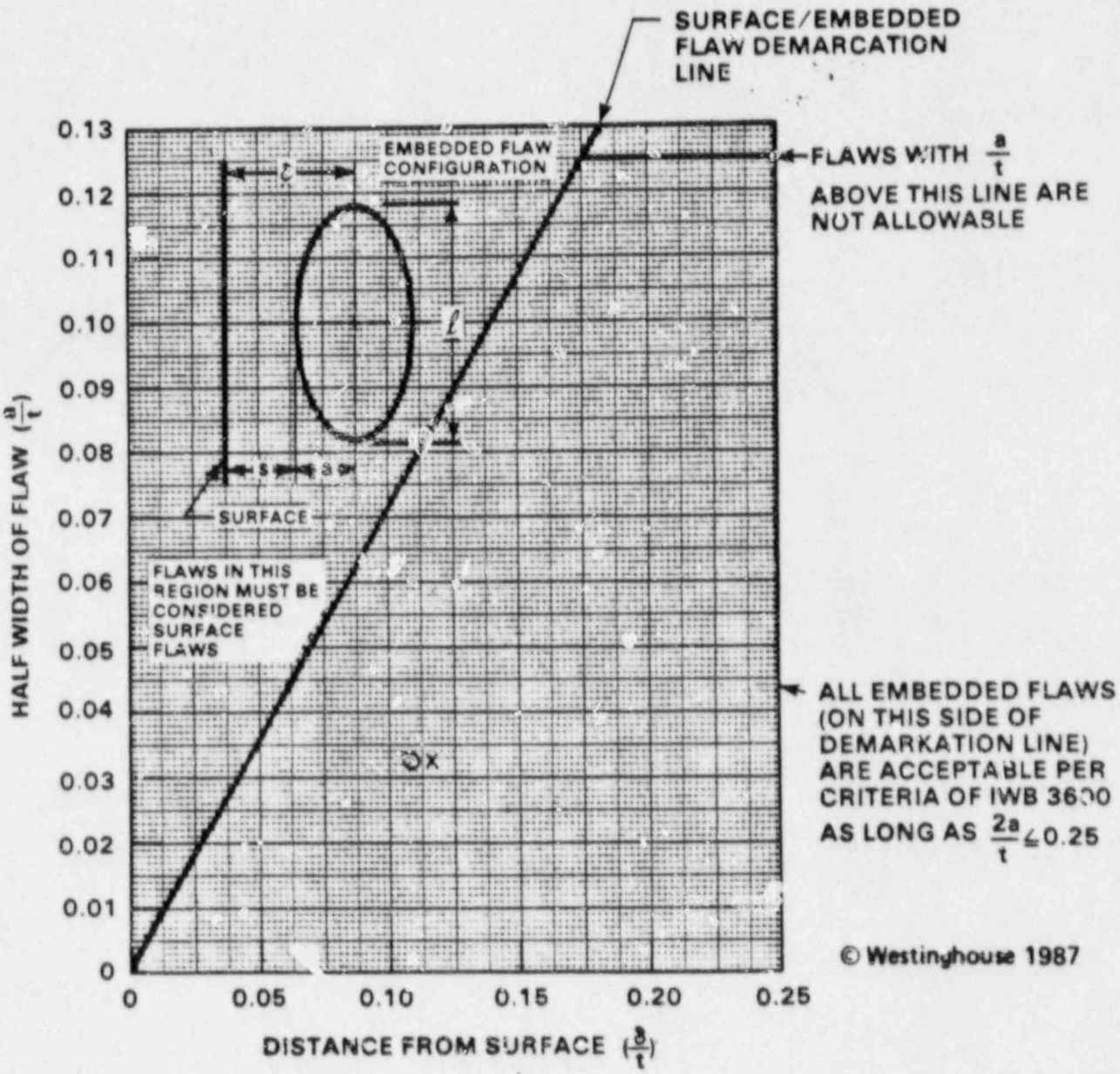

Figure 5-1 Embedded Flaw Evaluation Chart for Longitudinal and Circumferential Indications in the Reactor Vessel Outlet Nozzle to Shell Weld Region

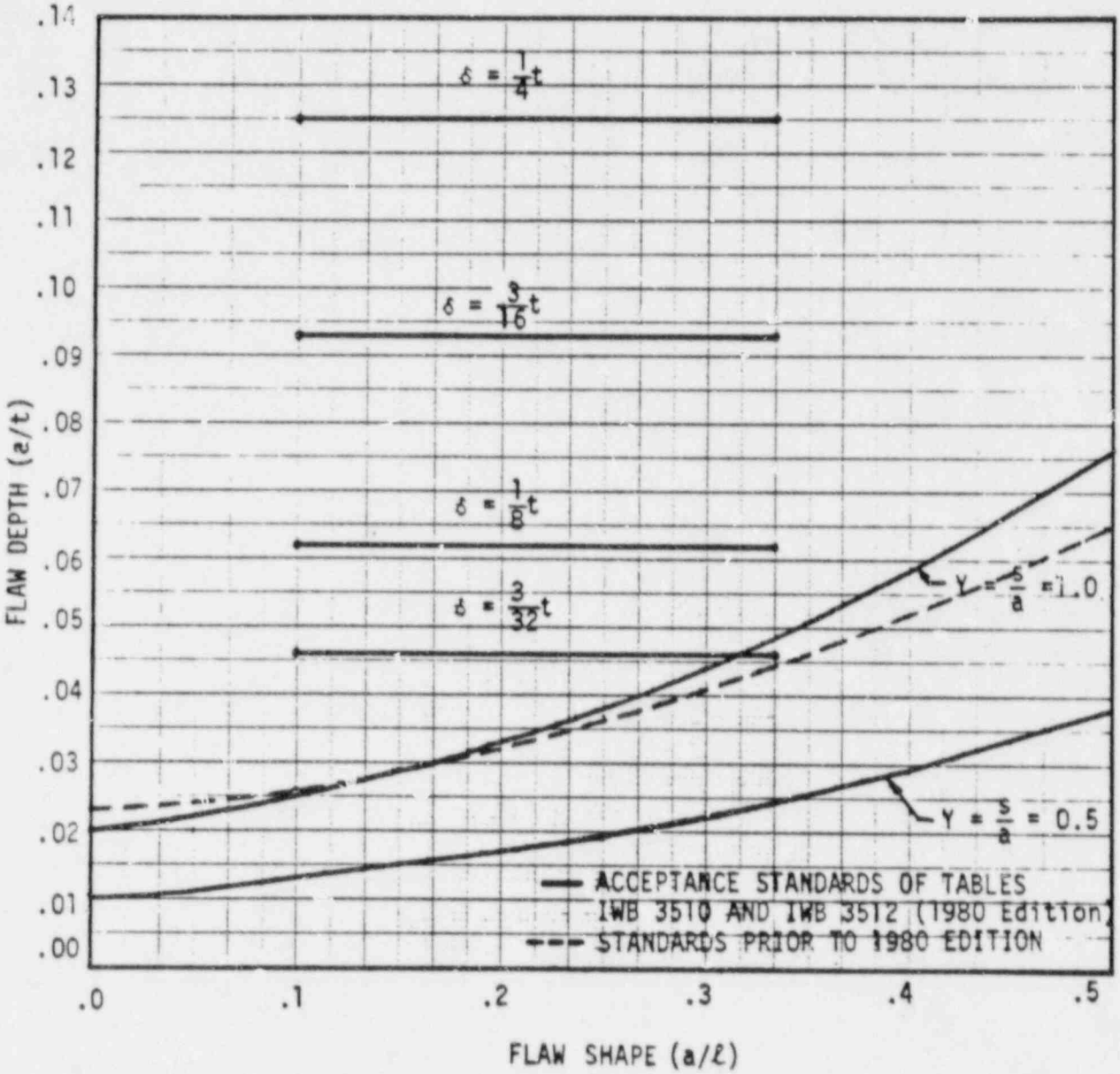

Figure 5-2 Acceptance Standards for Embedded Flaws, From Table IWB-3512-1

*Only Y = 1.0 curve applies to ASME Codes prior to 1980 Edition.

SECTION 6
REFERENCES

1. ASME Code Section XI, "Rules for Inservice Inspection of Nuclear Power Plant Components", 1980 Edition; 1983 and 1986 editions (used for updated standards tables, Section 4.5), and 1980 edition [Winter 1981 Addendum] (for revised reference crack growth curves).

2. Wren, J. R., and Sowers, M. G. "Analytical Report for Louisiana-Waterford Unit No. 3 Reactor Vessel" Combustion Engineering Nuclear Components Engineering Dept. Contract No. 74170 Report CENC-1259, June 1976.

3. "Project Specification for a Reactor Vessel Assembly for Waterford Unit 3" Combustion Engineering Inc., Windsor CT, Feb. 1976. Also "General Specification for a Reactor Vessel Assembly," number 00000-PE-110, August 1971.

4. "Evaluation of Pressurized Thermal Shock Effects Due to Small Break LOCA's with Loss of Feedwater for the Combustion Engineering NSSS" Combustion Engineering Inc. Report CEN-189, December, 1981.

5. Shelby, D. L., et. al. "Pressurized Thermal Shock Evaluation of the Calvert Cliffs Unit 1 Nuclear Power Plant" Oak Ridge National Labs Report ORNL/TM 9408, NUREG-CR 4022, September 1985.

6. Shah, R. C. and Kobayashi, A. S., "Stress Intensity Factor for an Elliptical Crack Under Arbitrary Loading", Engineering Fracture Mechanics, Vol. 3, 1981, pp. 71-96.

7. Lee, Y. S. and Bamford, W. H., "Stress Intensity Factor Solutions for a Longitudinal Buried Elliptical Flaw in a Cylinder Under Arbitrary Loads", presented at ASME Pressure Vessel and Piping Conference, Portland Oregon, June 1983. Paper 83-PVP-92.

8. Marston, T. U. et.al. "Flaw Evaluation Procedures: ASME Section XI" Electric Power Research Institute Report EPRI-NP-719-SR, August 1978.

9. "Final Safety Analysis Report: Waterford Unit 3" Combustion Engineering Report, 1976.

10. U.S. N.R.C Regulatory Guide 1.99, "Effects of Residual Elements on Predicting Radiation Damage to Nuclear Reactor Vessel Materials," July 1975; Rev. 1: April 1977, Rev. 2 (in press): February 1986.

11. Combustion Engineering Letter ESS-75-027 "Reactor Vessel Beltline Region for 157 inch and 172 inch Diameter Vessels." A. Ragl, January 13, 1975.

APPENDIX A

EVALUATION OF ULTRASONIC EXAMINATION INDICATIONS FOUND IN THE OUTLET NOZZLE TO SHELL WELD 01-021 SPRING, 1988

A-1.0 SUMMARY

During the Spring 1988 inservice ultrasonic examination of the Waterford Unit 3 reactor vessel outlet nozzle to shell weld number 01-021 three recordable indications were noted. Two of these were detected with a 0 degree, 2.25 MHz longitudinal wave examination from the nozzle bore, and the remaining one was detected with a 20 degree, 2.25 MHz longitudinal wave examination from the nozzle bore. These indications are clearly located within the weld at or near the weld/nozzle forging fusion line. An evaluation of these indications (using 50% DAC sizing criteria) to the acceptance standards in table IWB-3512-1 of the ASME Code Section XI, 1980 Edition through the 1981 Winter Addenda results in the two 0 degree longitudinal wave indications being acceptable. The 20 degree longitudinal wave indication exceeds the allowable limits of table IWB-3512-1.

In an effort to further characterize these indications, especially the 20 degree longitudinal wave indication, supplemental examinations were performed using the Dynacon Ultrasonic Data Recording and Processing System (UDRPS) with the standard inservice inspection transducers. With UDRPS these indications appeared to be rounded, volumetric-type reflectors most probably deposited during the fabrication welding process. An evaluation of these indications (using 6 dB drop sizing rather than 50% DAC sizing) to the acceptance standards in table IWB-3512-1 of the ASME Section XI, 1980 Edition through the 1981 Winter Addenda results in all three indications exceeding the allowable limits.

Using the fracture analysis rules of IWB-3600 and the guidelines of Appendix A both from the ASME Code Section XI, 1980 Edition through the 1981 Winter Addenda, all the indications are acceptable using the 50% DAC sizing levels with the conventional inservice examination and the 6 dB drop sizing levels with the UDRPS examinations.

A-2.0 WELD LOCATION

Weld No. 01-021 is the hot leg (outlet) nozzle to shell weld located at 0° vessel axis which is shown in the plan view and nozzle detail drawing, figures A.1 and A.2, respectively.

A-3.0 CONVENTIONAL ULTRASONIC EXAMINATIONS

Indication 1A was detected and measured with transducer TR 13, which is affixed to the RV-ISI-40 month array plate, figure A.3. Transducer TR 13 is mounted on the centerline of the array plate, directing the incident beam axially with respect to the nozzle bore, down to the weld area at a refracted angle in the longitudinal mode at 20°. When considering the nozzle taper angle of 5°, the interrogating beam is approximately 15° from the normal to the weld. Indications 1BB and 2CC were detected and measured with transducer TR 6, which is also positioned on the RV-ISI-40 month array plate centerline, directing the incident beam axially with respect to the nozzle bore, down to the weld area but at a refracted angle in the longitudinal mode of 6°. Considering the nozzle taper of 5°, the interrogating beam is essentially normal to the weld.

Supplemental examinations were conducted with transducer TR 5, which is positioned on the centerline of the 40 month array plate, directing the incident beam axially with respect to the nozzle bore, down to the weld at 45° in the shear mode. Considering the nozzle taper, the resulting interrogating beam is approximately 40° from the normal to the weld. For the purposes of this report, TR 6 will be referred to as the 0° beam, TR 13 will be called the 20° beam and TR 5 will be called the 45° beam.

Results of the conventional data for indication 1A are summarized in table A.1 and shown in figure A.4. Data for indications 1BB and 2CC, which were determined to be acceptable by the conventional ultrasonic examinations are included in table A.1. The location of indications 1BB and 2CC with respect to the weld cross-section and the nozzle azimuth are shown in figures A.5 and A.6, respectively.

Using flaw indication evaluation rules of IWA-3000 and the acceptance standards for flaw indications of IWB-3000 (specifically table IWB-3512-1 of the ASME Code Section XI, 1980 Edition through the 1981 Winter Addenda), it was determined that indication 1A has an actual a/t value of 5.54% compared to an allowable of 2.8%, indication 1BB has an actual a/t value of 4.56% compared to an allowable a/t of 5.2%, and indication 2CC has an actual a/t value of 2.05% compared to an allowable a/t of 4.1% (table A.1). Indications 1BB and 2CC are acceptable. Indication 1A exceeds the allowable limits.

A-4.0 REVIEW OF FABRICATION RADIOGRAPHS

Construction radiographs of the Waterford Unit 3 reactor vessel outlet nozzle to upper shell weld 01-021 were reviewed by qualified personnel in an effort to establish whether or not a correlation exists between the 1988 conventional ultrasonic examination data and results from the 1974 radiographic examination. The radiographic technique for the nozzle weld configuration specified the use of Kodak "AA" and "T" film in a double loaded cassette, placed on the inside diameter, with the high-energy x-ray source positioned essentially normal to the film and located outside the vessel. No relevant flaw-type images were noticeable on the construction radiographs in the area of interest. No flaw images were observed in all the radiographic film sets for weld 01-021.

A-5.0 BASELINE ULTRASONIC EXAMINATION RESULTS

An automated post-hydrostatic examination was performed at the fabrication shop in 1976. Techniques for examination of nozzle to shell weld 01-021 specified the use of 5° and 20° refracted longitudinal beams in a contact technique from the nozzle inner diameter bore. No recordable indications were noted in weld 01-021 during the baseline examination. Recording criteria was specified to be 50% of DAC.

A-6.0 SUPPLEMENTAL EXAMINATIONS WITH UDRPS

In order to obtain better information regarding the nature and size of the ultrasonic indication which exceeded the ASME Code Section XI table IWB-3512-1 using conventional ultrasonic examination data (indication 1A), it was decided to utilize the Dynacon Ultrasonic Data Recording and Processing System (UDRPS) with the conventional inservice inspection transducers. For information purposes it was also decided to utilize the UDRPS system on the two acceptable indications as identified on table A.1 (indications 1BB and 2CC). The UDRPS system is a known automated data recording and processing system which has the capability of recording, storing, processing and imaging ultrasonic test data. It allows for more extensive recording of data, better visualization of examination data through the use of color-coded images, more flexible manipulation of data, more consistent examination quality and archival retrieval of past examinations for comparison purposes.

The best use of the UDRPS data is the ability to observe secondary responses and their relationship to the primary signals from the indications. This aids in the characterization of the reflectors as well as potentially providing more accurate sizing information.

Characterization is defined as "the determination of whether a valid indication originates from a volumetric or planar type defect". Generally, the use of supplemental straight beam and angle beam techniques provide for the verification of a volumetric type flaw, i.e. slag, porosity, since a relatively strong reflection should occur from both.

Another supplemental characterization technique is based on satellite pulse observation technique (SPOT) principles [reference 1]. SPOT relies on the observation of a doublet signal emanating from a volumetric defect. This doublet consists of a strong specularly reflected signal, followed by a weak, synchronous satellite pulse response. This satellite pulse is created by a portion of the sound beam propagating around the circumference of a rounded type of reflector and being reradiated back to the receiver transducer. Synchronous means that when the specularly reflected signal peaks the

associated satellite pulse signal should also peak with the satellite pulse lagging in arrival time. Therefore these two peaks should occur in the same A-scan. On a system such as UDRPS two relatively close parallel images one behind the other would be indicative of synchronous signals and therefore a rounded volumetric type of defect.

For planar flaws, SPOT also relies on the observation of a doublet signal but these signals are asynchronous in nature. In this case the satellite responses are created by a portion of the sound beam being reradiated from a planar flaw extremity back to the receiver transducer. Since the extremities of planar flaws are separated in position the peaks of each extremity would not occur in the same A-scan. On a system such as UDRPS two parallel images but shifted in position would be indicative of asynchronous signals and therefore a planar type of defect.

UDRPS was also used to determine the reflector's sizes using amplitude drop sizing methods. The UDRPS system, however, has the same fallacies as conventional ultrasonic examination techniques when amplitude drop sizing methodologies are used. For small flaws it will still provide estimated sizes more commensurate with the beam size of the transducer rather than the size of the flaw, assuming as in most cases that the beam size is greater than the size of the flaw [references 1-5].

With this in mind, for these indications a sizing methodology known as 6 dB drop or half maximum amplitude was applied. This methodology was applied because overall (on a defect matrix consisting of volumetric and planar type flaws) it has been shown to provide the more accurate results when compared to other amplitude-based techniques such as 50% DAC, 20% DAC, and 20% DAC with beam spread correction [reference 6].

Indication 1A found during the conventional inservice inspection was re-examined using UDRPS and the Westinghouse 40-month array plate. The transducer which detected this indication is a 2.25 MHz, 1-1/2 inches diameter, 20 degree longitudinal wave unit identified as TR 13. This same transducer was used in the UDRPS scans. Other angles/transducers were also

used to obtain supplemental information on this indication. These additional units included TR 6 which transmits essentially a 0 degree longitudinal wave with respect to the weld fusion line and TR 5 which transmits a 45° shear wave from the nozzle bore. For the UDRPS examinations, six scans (two for each angle/transducer) were performed on this indication. Each of the scans were conducted in a raster fashion using the Y-axis of the mechanized scanner (toward and away from the reactor vessel centerline) as the scanning axis and using the B-axis of the mechanized scanner (around the nozzle bore) as the indexing axis. Each index was 0.5 degrees (excluding one TR 6 scan in which an increment of 0.33 degrees was used) around the nozzle or a 0.31 inch increment at the location of the indication. The first UDRPS scan for each angle/transducer was performed at the sensitivity required to achieve a maximum amplitude of 80% full screen height from the indication of interest. The remaining scan for each angle/transducer was performed at a sensitivity ranging from 8 to 10 dB above the first scan level. This higher sensitivity scan was performed to try to distinguish secondary responses which could determine the nature of the indication. The lower sensitivity scan was performed to enable a 6 dB drop sizing methodology to be applied. For all supplemental UDRPS investigations, distance amplitude correction circuitry was not utilized.

The results of these examinations can best be observed in figures A.7 through A.13. A brief explanation of each of these figures is provided below:

Figure A.7: Indication 1A in Outlet Nozzle to Shell Weld 01-021 With Respect to a Weld Cross-section (Transducer TR 13 - Low Sensitivity Scan), UDRPS Data - Sweep with Maximum Amplitude from Reflector

This image is of the scan line which showed the maximum response from indication 1A. For clarity and illustration purposes the estimated positions of the shell, weld and nozzle are shown. Indication 1A appears to be near the weld/nozzle forging fusion line and clearly embedded within the weld. Using 6 dB drop sizing the through-wall dimension (2a) of indication 1A using TR 13 is determined to be 0.743 inch. This dimension is shown on the figure.

Figure A.8: Linear Extent of Indication 1A in Outlet Nozzle to Shell Weld 01-021 (Transducer TR 13 - Low Sensitivity Scan), UDRPS Data

The series of images shown on this figure display the linear extent of indication 1A without any amplitude drop type sizing. Using 6 dB drop sizing indication 1A can be seen ranging from 347.5 to 354.0 degrees or 14 increments. Each increment was 0.5 degrees therefore the indication extends approximately 7 degrees. Each degree at the position of the weld/nozzle fusion line is equal to 0.61 inch (diameter equals 70.06 inches). Therefore indication 1A by 6 dB drop sizing measures 4.27 inches.

Figure A.9: Secondary Image of Indication 1A (Transducer TR 13 - High Sensitivity Scan), UDRPS Data - Sweep With Maximum Amplitude from Reflector

This image shows a saturated response from indication 1A as well as a weak trailing secondary response approximately 3.5 microseconds behind the primary indication 1A response. These responses are indicated on the figure. Trailing secondary responses are evidence of rounded volumetric-type reflectors.

Figure A.10: Indication 1A in Outlet Nozzle to Shell Weld 01-021 With Respect to the Weld Cross-section (Transducer TR 6 - Low Sensitivity Scan), UDRPS Data - Sweep With Maximum Amplitude from Reflector

This image is of the scan line which showed the maximum response from indication 1A using TR 6. Estimated positions of the shell, weld and nozzle are shown for clarity and illustration purposes. Indication 1A appears to be two separate reflectors (approximately 1.6 inches between peak amplitude positions) located at or near the weld/nozzle forging fusion line and embedded within the weld. Using 6 dB drop sizing and ASME Code Section XI IWA-3300 flaw indication proximity rules the through-wall dimension (2a) of indication 1A using TR 6 is determined to be 2.48 inches (0.59 inch for one reflector

plus the separation distance of 0.5 inch plus 1.4 inches for the other reflector). This dimension is shown on the figure. Trailing secondary responses can be observed for both reflectors.

Figure A.11: Linear Extent of Indication 1A (Transducer TR 6 - Low Sensitivity Scan), UDRPS Data

The series of images shown on this figure display the linear extent of indication 1A using TR 6 without any amplitude drop type sizing. Using 6 dB drop sizing indication 1A can be seen ranging from 352.56 - 353.55 degrees or 4 increments. Each increment was 0.33 degree therefore the indication extends approximately 1.32 degrees. Indication 1A using TR 6 and 6 dB drop sizing measures 0.81 inch in length.

Figure A.12: Secondary Images of Indication 1A (Transducer TR 6 - High Sensitivity Scan), UDRPS Data - Sweep with Maximum Amplitude from Reflector

This image shows a saturated response from indication 1A using TR 6 as well as a weak trailing secondary response approximately 3.0 microseconds behind the primary indication 1A response. These responses are indicated on the figure. Trailing secondary responses are evidence of rounded volumetric-type reflectors.

Figure A.13: Linear Extent of Indication 1A (Transducer TR 5 - Low Sensitivity Scan), UDRPS Data

The series of images shown on this figure display the linear extent of indication 1A using TR 5 without any amplitude drop type sizing. Two reflectors approximately 0.9 inch apart are present. Using 6 dB drop sizing indication 1A can be seen ranging from 350.5 to 354.0 degrees or 8 increments. Each increment was 0.5 degrees therefore the indication extends approximately 4 degrees. Indication 1A using TR 5 and 6 dB drop sizing measures 2.44 inches in length.

For information purposes, the two indications identified as 1BB and 2CC which were determined to be acceptable to table IWB-3512-1 of the ASME Code Section XI using the conventional ultrasonic examination data were re-examined using UDRPS and the Westinghouse 40-month array plate. The transducer which detected these indications is a 2.25 MHz, 1-1/2 inches diameter, 0 degree longitudinal wave (with respect to the weld fusion line) unit identified as TR 6. This same transducer was used in the UDRPS scans. The same type of scanning scheme used for indication 1A was applied to these two indications except that the index increment was 0.33 degrees around the nozzle or a 0.2 inch increment at the location of the indication and only the detection transducer was used.

The results of these examinations can best be observed in figures A.14 through A.17. A brief explanation of each of these figures is provided below:

Figure A.14: Indication 1BB in Outlet Nozzle to Shell Weld 01-021 With Respect to Weld Cross-section (Transducer TR 6 - Low Sensitivity Scan), UDRPS Data - Sweep with Maximum Amplitude from Reflector

This image is of the scan line which showed the maximum response from indication 1BB. Estimated positions of the shell, weld and nozzle are shown for clarity and illustration purposes. Indication 1BB appears to be two reflectors (approximately 0.9 inch between peak amplitude positions) located at or near the weld/nozzle forging fusion line and embedded within the weld. Using 6 dB drop sizing and ASME Code Section XI IWA-3300 flaw indication proximity rules, the through-wall dimension (2a) of indication 1BB is determined to be 2.02 inches. This dimension is shown on the figure.

Figure A.15: Linear Extent of Indication 1BB (Transducer TR 6 - Low Sensitivity Scan), UDRPS Data

The series of images shown on this figure display the linear extent of indication 1BB without any amplitude drop type sizing. Using 6 dB drop sizing and ASME Code Section XI IWA-3300 flaw indication proximity rules, indication 1BB

can be seen from 29.31 to 32.94 degrees or 13 increments. Each increment was 0.33 degrees therefore the indication extends approximately 4.29 degrees in length or 2.62 inches.

Figure A.16: Indication 2CC in Outlet Nozzle to Shell Weld 01-021 With Respect to the Weld Cross-section (Transducer TR 6 - Low Sensitivity Scan), UDRPS Data - Sweep With Maximum Amplitude from Reflector

This image is of the scan line which showed the maximum response from indication 2CC. Estimated positions of the shell, weld and nozzle are shown for clarity and illustration purposes. Indication 2CC appears to be two reflectors (approximately 1 inch between peak amplitude positions) located at or near the weld/nozzle forging fusion line and embedded within the weld. Using 6 dB drop sizing and ASME Code Section XI IWA-3300 flaw indication proximity rules, the through-wall dimension (2a) of indication 2CC is determined to be 1.75 inches. This dimension is shown on the figure.

Figure A.17: Linear Extent of Indication 2CC (Transducer TR 6 - Low Sensitivity Scan), UDRPS Data

The series of images shown on this figure display the linear extent of indication 2CC without any amplitude drop type sizing. Using 6 dB drop sizing, indication 2CC can be seen ranging from 298.72 to 302.35 degrees or 12 increments. Each increment is 0.33 degrees therefore the indication extends approximately 3.96 degrees in length or 2.42 inches.

The UDRPS sizing information using 6 dB drop sizing techniques for indications 1A, 1BB and 2CC of weld 01-021 are summarized in table A.2. Flaw indication analyses in accordance with Section XI IWA-3300 and IWB-3512 for each of the indications using the UDRPS sizing data are also included in table A.2. Each of the angle/transducer combinations used on indications 1A, 1BB, and 2CC resulted in flaw indication sizes exceeding the allowable limits of table IWB-3512-1. In comparison with the conventional inservice inspection results on these indications (table A.1) the UDRPS 6 dB amplitude drop sizing

dimensions are consistently greater with the exception of the 20 degree longitudinal wave inspection results. These results can be explained by the variation in sizing techniques, i.e. conventional 50% DAC as compared to 6 dB drop. In conventional 50% DAC sizing, the reference line (100% DAC line) is established on a side-drilled hole or a series of side-drilled holes at distances representative of the examination value. Indications located within the outer 75% of the through thickness of the weld exceeding 50% of this reference line are sized. These indications are dimensioned by measuring the area over which the response from the indications equal or exceed the 50% DAC level. In most applications the higher the amplitude the greater the ultrasonically measured size of the indication irrespective of the true size of the reflector. Measured size, therefore, is dependent on the comparative reflectivity of the flaw indication. If reflectors adjacent to the recorded indications are below the 50% DAC level they are not included in the size.

In the 6 dB drop sizing performed in this application, the maximum amplitude response from the indication is arbitrarily set at approximately 80% full screen height thereby establishing a reference from the reflector itself and ignoring a comparison with the response from a side-drilled hole. All indications of interest exceeding approximately 40% full screen height are dimensioned. This dimensioning is performed by measuring the area over which the response from each reflector equals or exceeds half the maximum reflector response. Therefore if reflectors adjacent to the recorded indications are greater than 40% full screen height they are dimensioned and included in the evaluation. This methodology, by definition, will yield large sizes for indications less than 100% DAC during the conventional examinations since no minimum level such as 50% DAC is adhered to, and by arbitrarily increasing the gain, adjacent reflectors may also have to be included. These sizes, however, are still commensurate with the beam spread of the transducer rather than the true reflector size at least when concerned with small volumetric reflectors.

In terms of specifics, UDRPS 6 dB drop sizing data for indication 1A, using transducers TR 6 and TR 5 was obtained at gain settings which were approximately two times the conventional examination reference sensitivity. This resulted in the combined measurement and subsequent assessment of two adjacent

reflectors which were at or below the recording level in the conventional examinations. In the UDRPS 6 dB drop sizing data for indications 1BB and 2CC, the proximity rules of Section XI were applied to smaller amplitude adjacent reflectors even though the conventional UT measurements between 50% DAC points indicate that the recorded indications were singularly acceptable, and sufficiently separated from the adjacent reflectors noticed in the UDRPS examinations.

In summary, indications 1A, 1BB and 2CC using UDRPS data are interpreted to be rounded, volumetric type reflectors that are clearly subsurface in nature and are located at or near the weld/nozzle forging interface.

A-7.0 FRACTURE MECHANICS EVALUATION

The three indications (1A, 1BB, 2CC) found in weld No. 01-021 have been evaluated by a fracture mechanics analysis using the flaw chart developed in the main body of this report, and both conventional ultrasonic examination and UDRPS examination sizing data (table A.1 and table A.2). This evaluation is provided in figure A.18 for indications 1A, 1BB, and 2CC.

All the indications identified by both the conventional ultrasonic examinations and the UDRPS examinations are acceptable by the fracture mechanics analysis.

A-8.0 REFERENCES

1. Gruber, G. J., G. J. Hendrix, and W. R. Schick. "Characterization of Flaws in Piping Welds Using Satellite Pulses," Materials Evaluation, Volume 42, April 1984, pp. 426-432.

2. Cook, R. V., P. J. Latimer, and R. W. McClung. Flaw Measurement Using Ultrasonics in Thick Pressure Vessel Steel, Final Report on Contract No. W-7405-eng-26, prepared by Oak Ridge National Laboratory for the U. S. Nuclear Regulatory Commission, August 1982, Oak Ridge, TN.

3. Doctor, S. R., et al. "Effectiveness of U. S. Inservice Inspection Techniques - A Round Robin Test ", Proceedings of Specialist Meeting on Defect Detection and Sizing, Ispra, Italy, May 3-6, 1983.

4. Jessop, T. J., P. J. Mudge, and J. D. Harrison. Ultrasonic Measurement of Weld Flaw Size, National Cooperative Highway Research Program Report 242, prepared for the Transportation Research Board by The Welding Institute, December 1981.

5. Mudge, P. J., and T. J. Jessop. "Size Measurement and Characterization of Weld Defects by Ultrasonic Testing: Findings of a Collaborative Programme", Proceedings of NDE in Relation to Structural Integrity, Paris, France, August 24-25, 1981.

6. Willetts, A. J., F. V. Ammirato, and E. K. Kietzman, J. A. Jones Applied Research Company/EPRI NDE Center. Accuracy of Ultrasonic Flaw Sizing Techniques for Reactor Pressure Vessels, Draft Interim Report, LPRI RP 1570-2, March 1988.

TABLE A.1

CONVENTIONAL DATA, 1988 EXAMINATIONS
WELD 01-021 OUTLET NOZZLE TO SHELL AT 0°

Indication No.	1A	1BB	2CC
Search Unit	TR 13	TR 6	TR 6
Peak Radial Location From Vessel Centerline	94.67"	92.34"	88.02"
Upper Shell I.D. Radius	86"	86"	86"
Depth From Nozzle Bore	12.09"	12.06"	11.7"
Depth From O.D. Surface (S)*	2.73"	3.34"	4.01"
Peak Angular Location of Flaw (Nozzle Azimuth)**	347.32°	31.8°	300.88°
Length (l)****	4.61"	1.21"	.73"
Through Wall Dimension (2a)****	1.19"	.98"	.44"
Upper Shell Thickness Minus Cladding (t)	10.75"	10.75"	10.75"
Code Classification***	Subsurface	Subsurface	Subsurface
Aspect Ratio (a/l)	.13	.40	.30
a/t%	5.54	4.56	2.05
Allowable a/t%***	2.8	5.2	4.1

*Measured from scaled plots, figures A.4 through A.6.

**0 degree is top center of nozzle when viewed from reactor vessel centerline

***ASME Code Section XI, 1980 Edition through 1981 Winter Addenda

****50% DAC sizing

TABLE A.2

SUMMARY OF INDICATIONS IN OUTLET NOZZLE TO SHELL WELD 01-021
UDRPS DATA (6 dB DROP SIZING), 1988 EXAMINATIONS

Indication	1A	1A	1A	1BB	2CC
Search Unit	TR 13	TR 6	TR 5	TR 6	TR 6
Length (l)*	4.27"	0.81"	2.44"	2.62"	2.42"
Through Wall Dimension (2a)*	0.743"	2.49"	1.38"	2.02"	1.75"
Depth from O.D. Surface (S)**	2.73"	2.73"	2.73"	3.34"	4.01"
Upper Shell Thickness Minus Cladding (t)	10.75"	10.75"	10.75"	10.75"	10.75"
Code Classification***	Subsurface	Subsurface	Subsurface	Subsurface	Subsurface
"a"	0.37"	1.24"	0.69"	1.01"	0.88"
Aspect Ratio (a/l)	0.09	0.5	0.28	0.39	0.36
a/t%	3.4	11.5	6.4	9.4	8.2
Allowable a/t%***	2.6	6.5	3.9	5.2	4.6

*6 dB drop sizing

**Measured from scaled plots, figures A.4 through A.6

***ASME Code Section XI, 1980 Edition through 1981 Winter Addenda

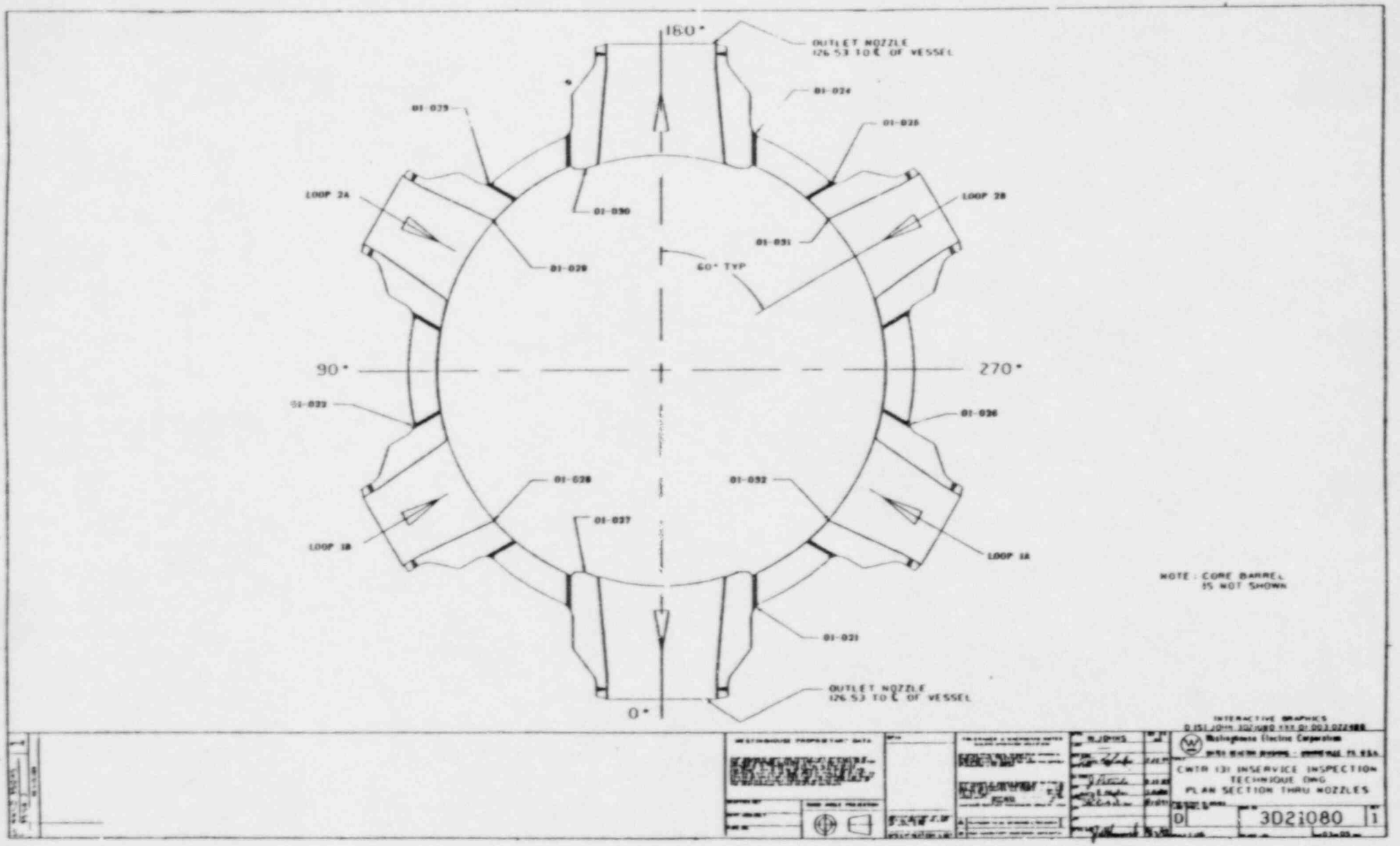

FIGURE A.1 : PLAN VIEW OF WATERFORD UNIT 3 REACTOR VESSEL THROUGH THE NOZZLES

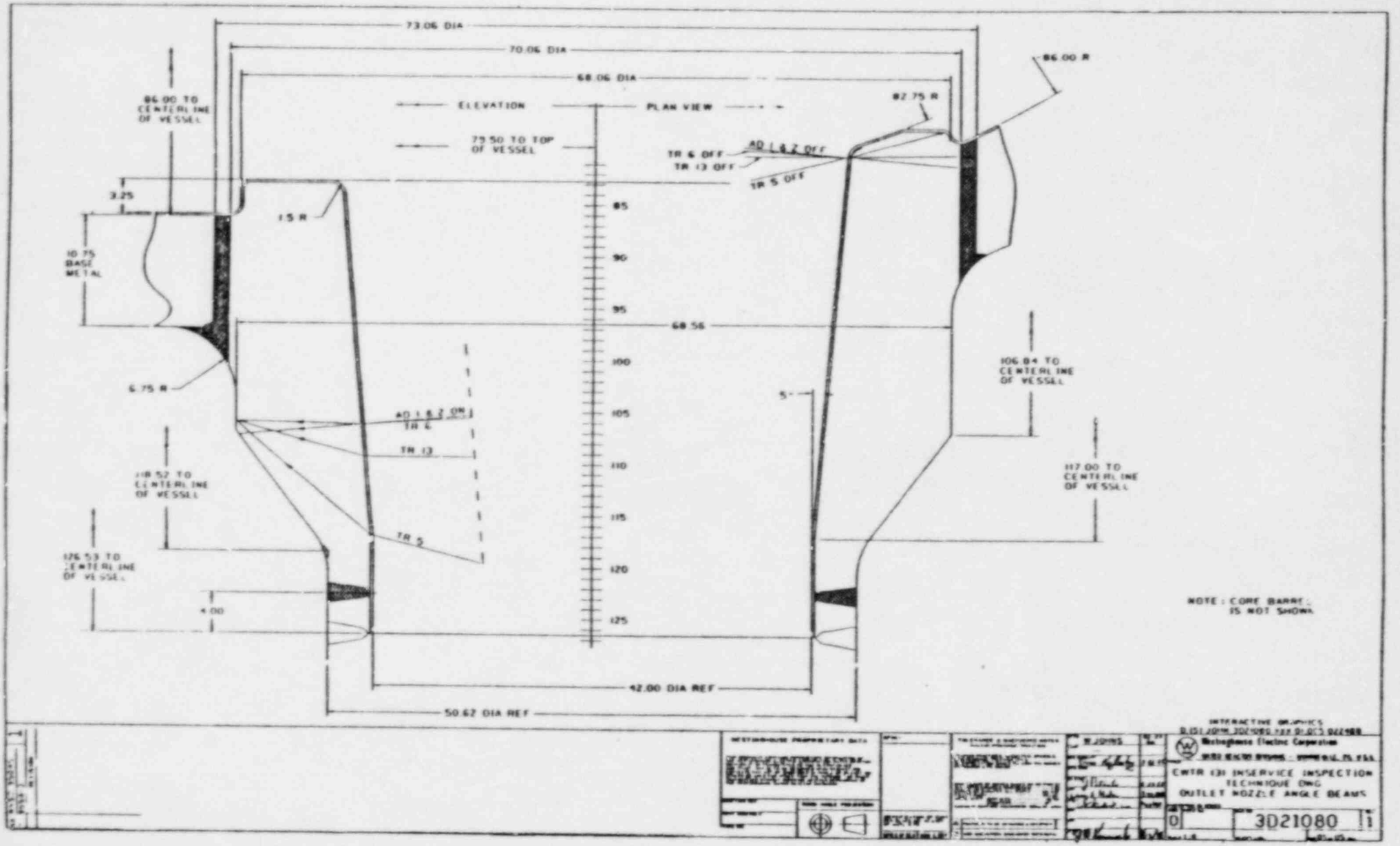

FIGURE A.2 : WATERFORD UNIT 3 OUTLET NOZZLE DETAIL DRAWING

FIGURE A.3 : WESTINGHOUSE REACTOR VESSEL-ISI 40-MONTH ARRAY PLATE FOR WATERFORD UNIT 3

WATERFORD UNIT # 3

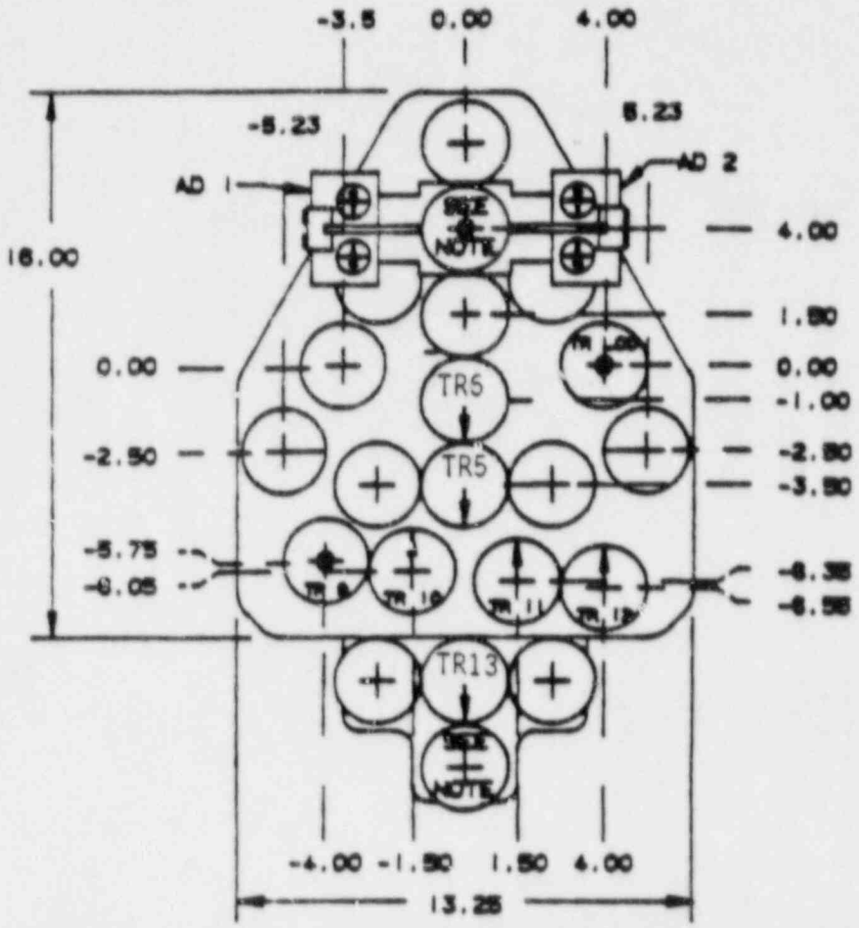

TRANSDUCER IDENTIFICATION NUMBER	NOMINAL INCIDENT ANGLE	NOMINAL REFRACTED ANGLE	TRANSDUCER MOUNT ANGLE (CALIBRATION)	TRANSDUCER MOUNT ANGLE (EXAMINATION)
AD 1	12.5°	60° L	12.5°	00.00°
AD 2	12.5°	60° L	12.5°	00.00°
TR 05	19°	45° S	19°	19°
TR 06	1.5°	6° L	1.5°	1.5°
TR 09	0°	0° L	0°	0°
TR 10	1.5°	6° L	1.5°	1.5°
TR 11	3°	12° L	3°	3°
TR 12	4°	16° L	4°	4°
TR 13	5°	20° L	5°	5°
TR L00	0°	0° L	0°	0°

NOTE: USED FOR PERPENDICULARITY ONLY.

RV-ISI 40 MONTH ARRAY PLATE

WESTINGHOUSE ELECTRIC CORPORATION

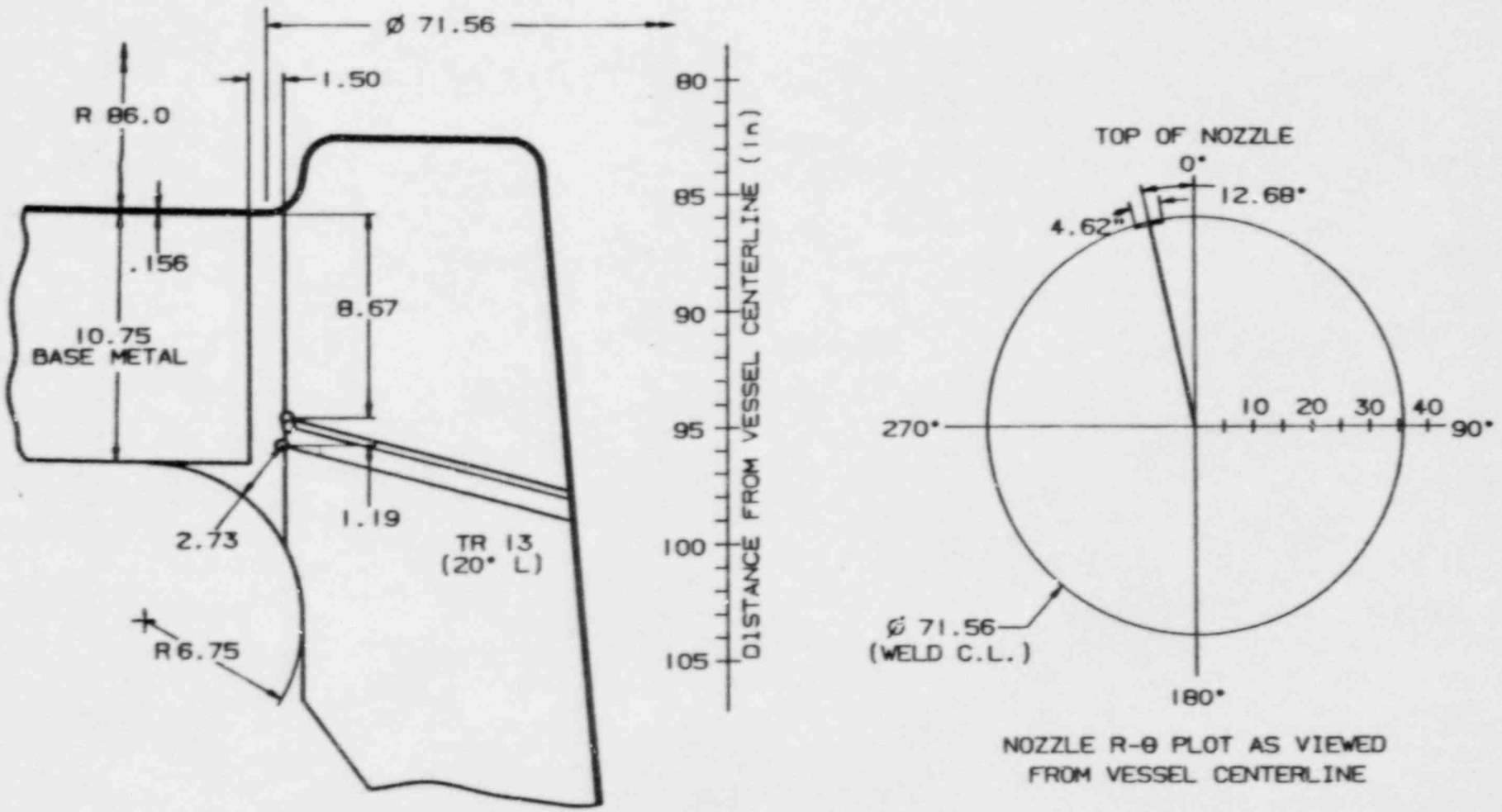

NOZZLE SECTION AT -12.68° (347.32°)

NOZZLE R-θ PLOT AS VIEWED FROM VESSEL CENTERLINE

WATERFORD UNIT •3 RV-ISI
OUTLET NOZZLE WELD 01- 021 INDICATION • 1A MAP

FIGURE A.4 : LOCATION OF INDICATION 1A IN OUTLET NOZZLE TO SHELL WELD 01-021, CONVENTIONAL ISI DATA

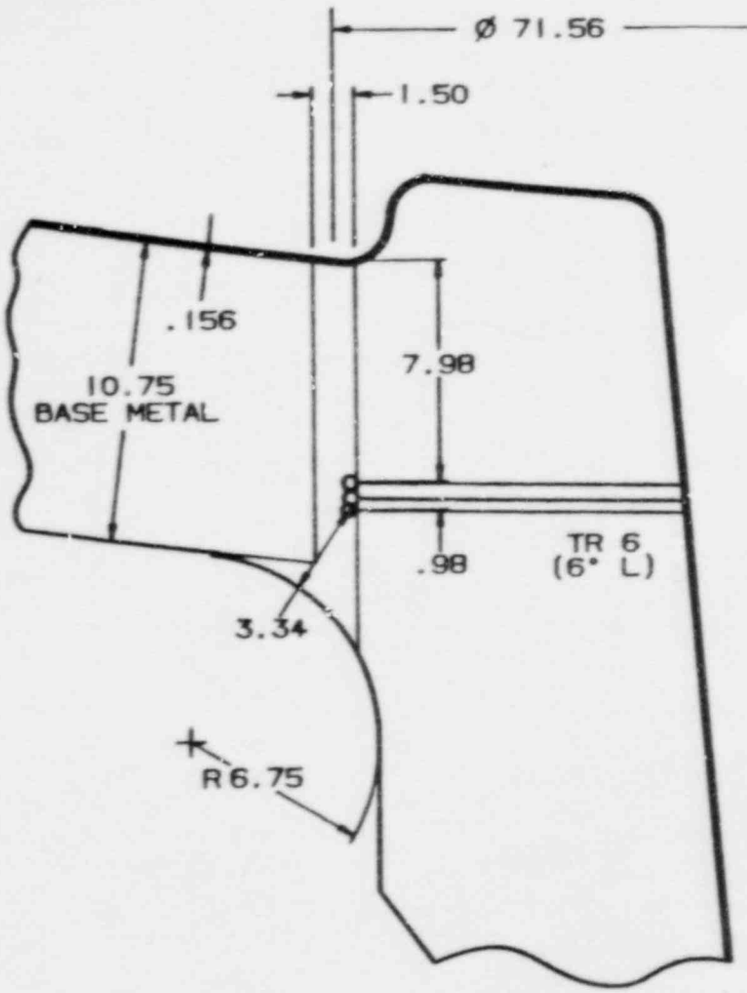

NOZZLE SECTION AT 31.80°

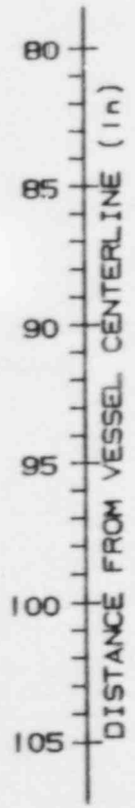

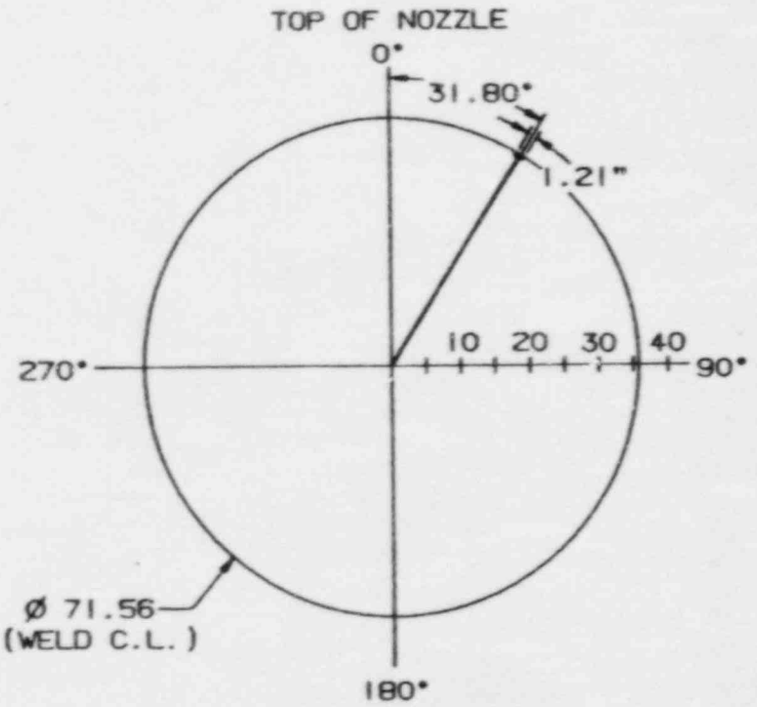

NOZZLE R-θ PLOT AS VIEWED
FROM VESSEL CENTERLINE

WATERFORD UNIT •3 RV-ISI
OUTLET NOZZLE WELD 01- 021 INDICATION • 1BB MAP

FIGURE A.5 : LOCATION OF INDICATION 1BB IN OUTLET NOZZLE TO SHELL WELD 01-021, CONVENTIONAL ISI DATA

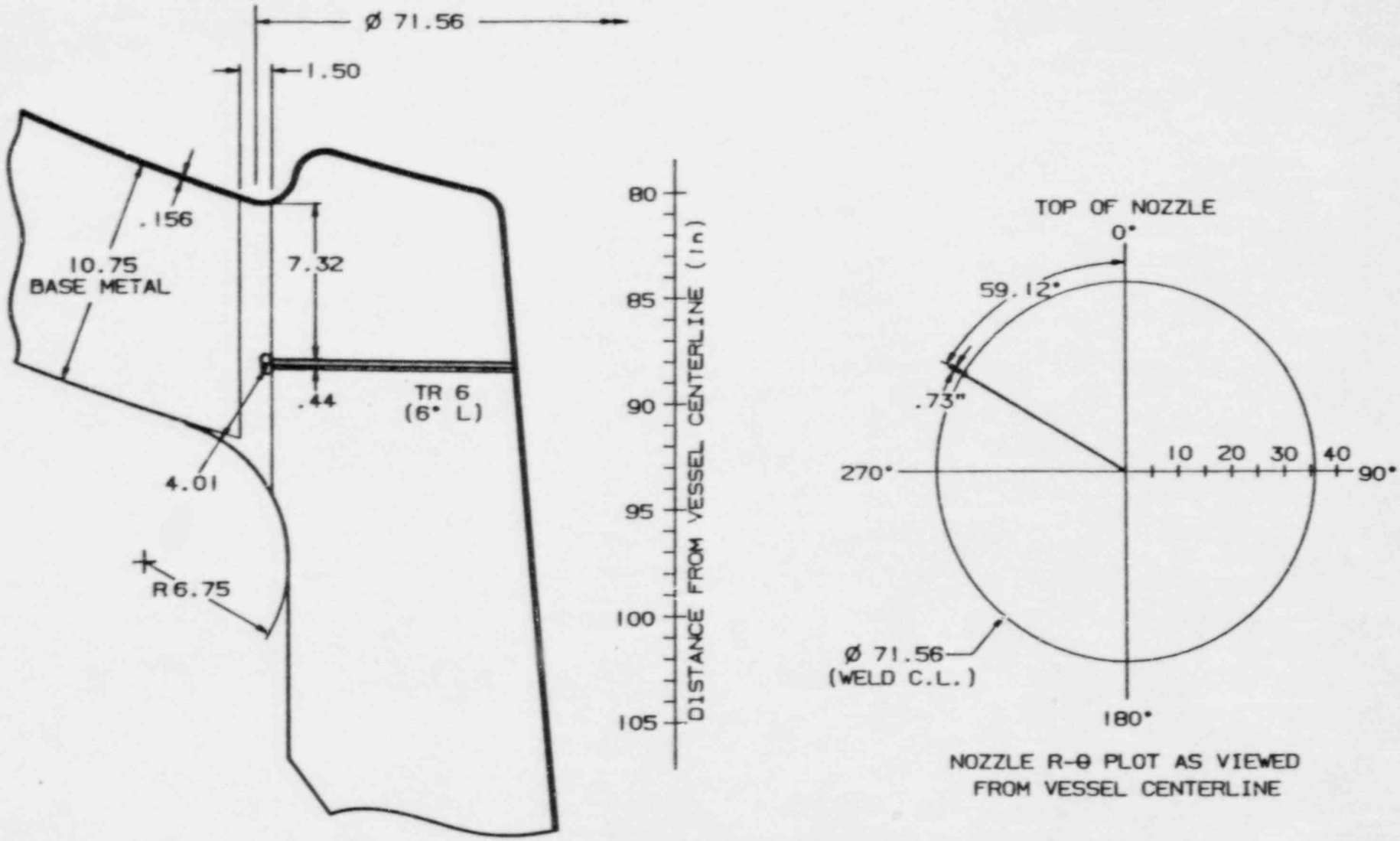

NOZZLE SECTION AT -59.12° (300.88°)

NOZZLE R-θ PLOT AS VIEWED FROM VESSEL CENTERLINE

WATERFORD UNIT •3 RV-ISI
OUTLET NOZZLE WELD 01- 021 INDICATION • 2CC MAP

FIGURE A.6 : LOCATION OF INDICATION 2CC IN OUTLET NOZZLE TO SHELL WELD 01-021, CONVENTIONAL ISI DATA

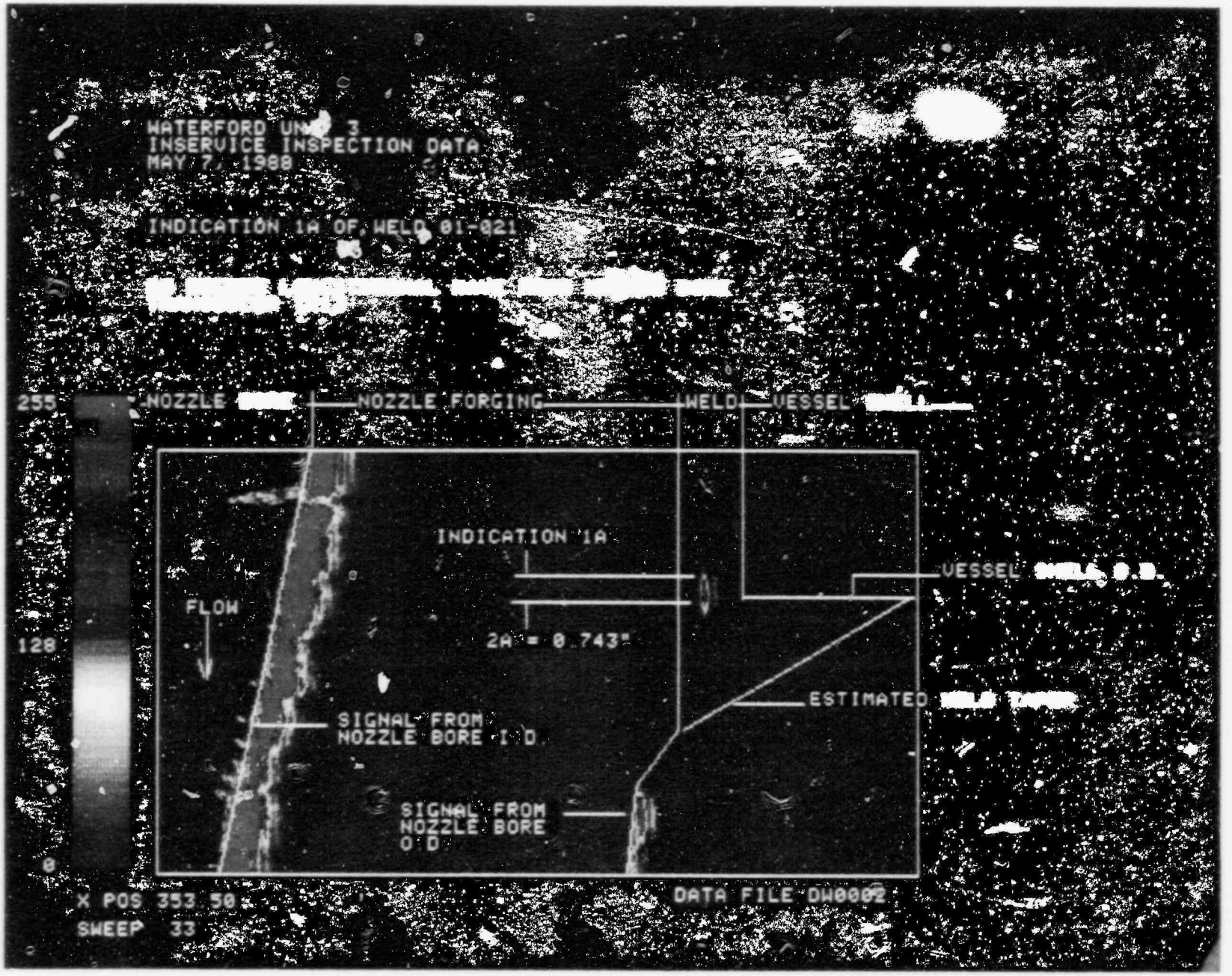

FIGURE A.7 : INDICATION 1A IN OUTLET NOZZLE TO SHELL WELD 01-021 WITH RESPECT TO A WELD CROSS-SECTION (TRANSDUCER TR 13 - LOW SENSITIVITY SCAN), UDRPS DATA - SWEEP WITH MAXIMUM AMPLITUDE FROM REFLECTOR

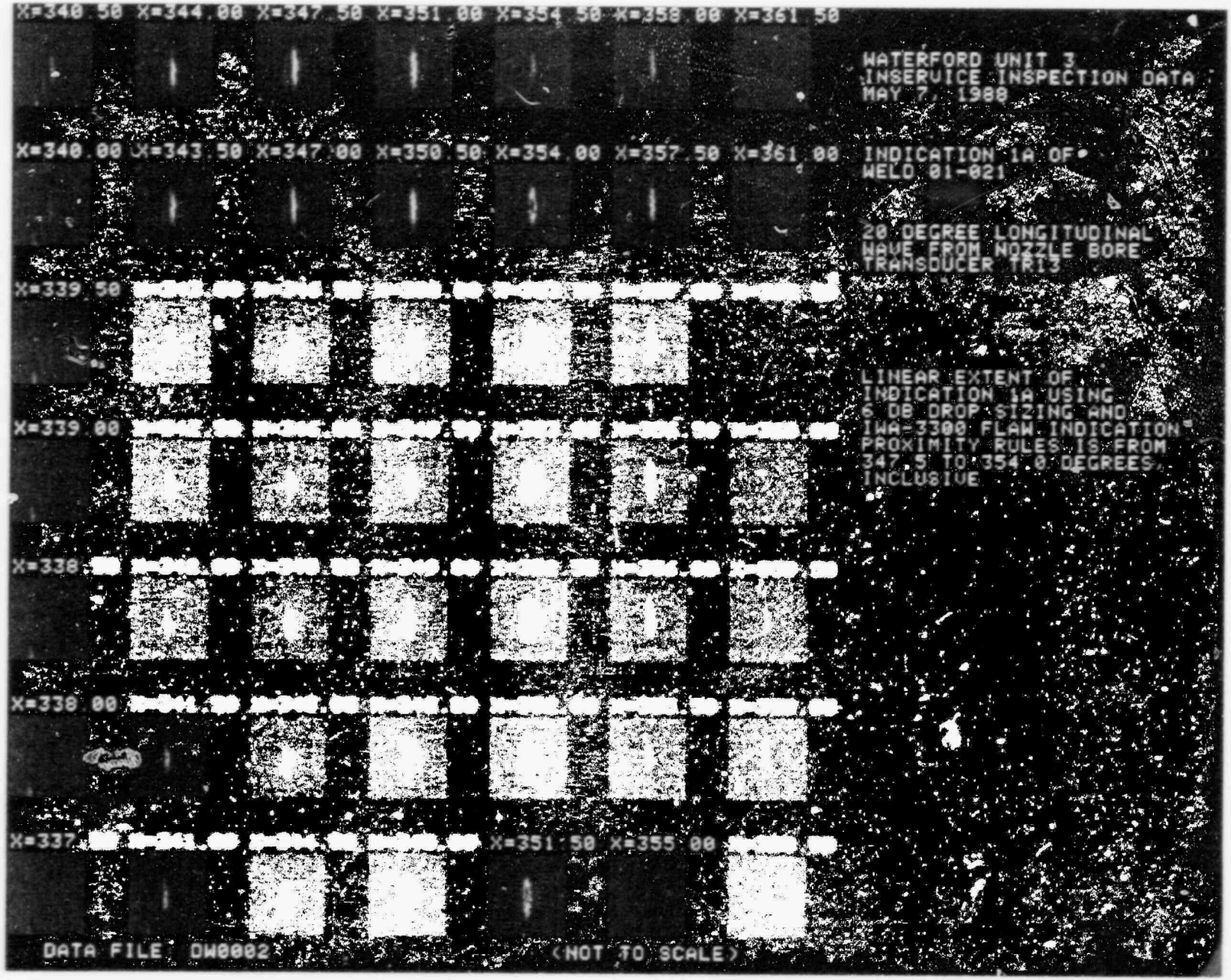

FIGURE A.8 : LINEAR EXTENT OF INDICATION 1A IN OUTLET NOZZLE TO SHELL WELD 01-021 (TRANSDUCER TR 13 - LOW SENSITIVITY SCAN), UDRPS DATA

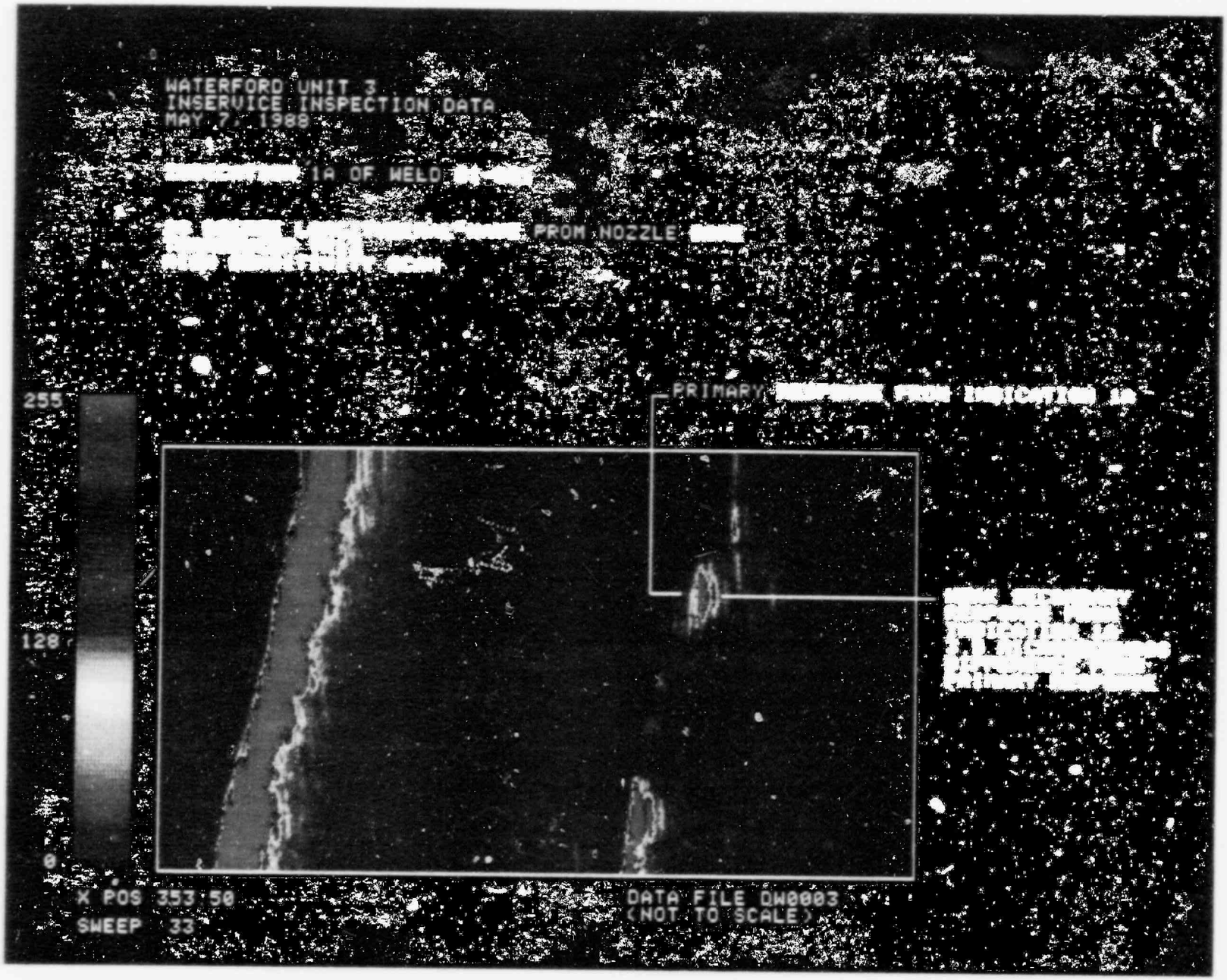

FIGURE A.9 : SECONDARY IMAGE OF INDICATION 1A (TRANSDUCER TR 13 - HIGH SENSITIVITY SCAN), UDRPS DATA - SWEEP WITH MAXIMUM AMPLITUDE FROM REFLECTOR

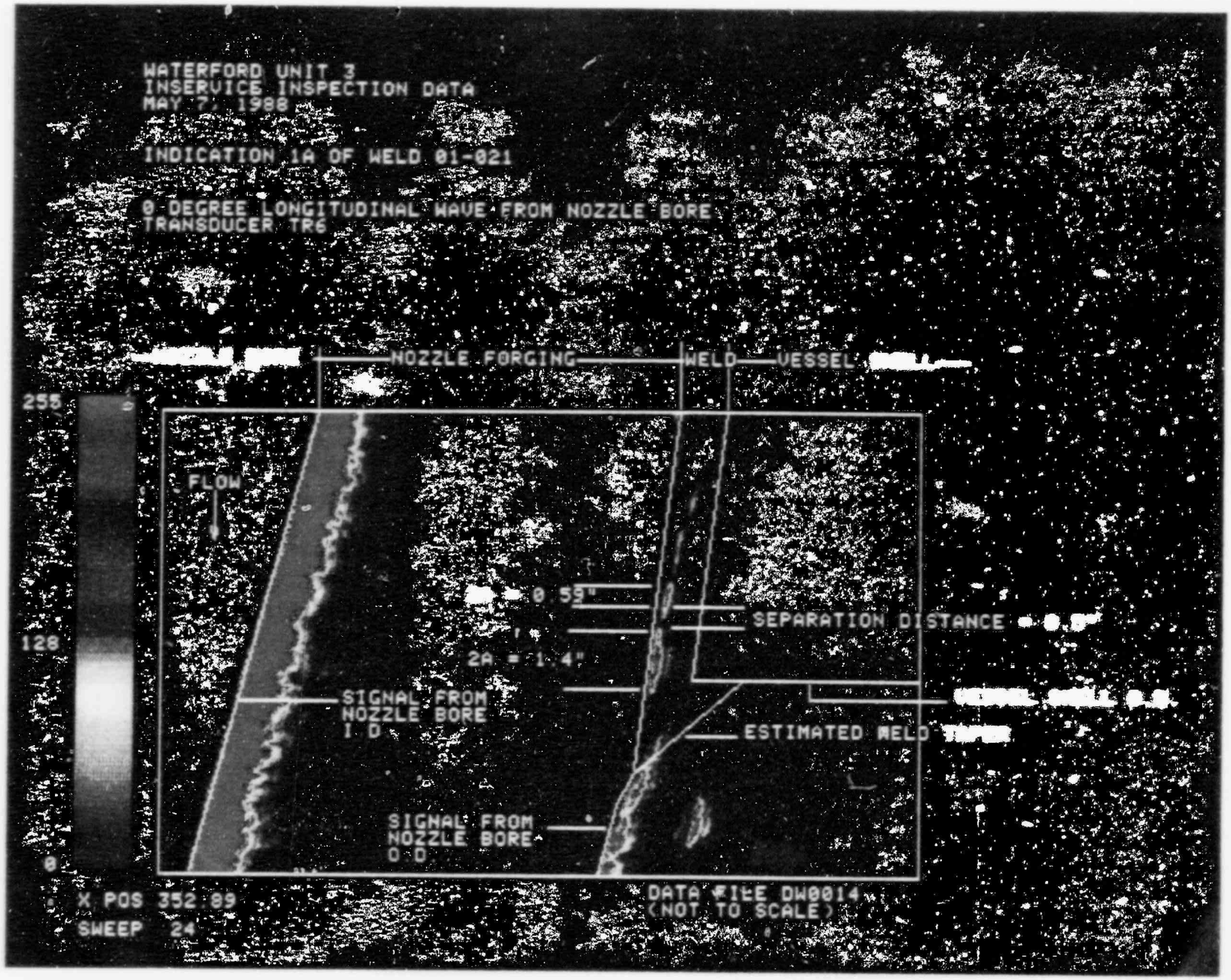

FIGURE A.10 : INDICATION 1A IN OUTLET NOZZLE TO SHELL WELD 01-021 WITH RESPECT TO WELD CROSS-SECTION (TRANSDUCER TR 6 - LOW SENSITIVITY SCAN), UDRPS DATA - SWEEP WITH MAXIMUM AMPLITUDE FROM REFLECTOR

FIGURE A.11 : LINEAR EXTENT OF INDICATION 1A (TRANSDUCER TR 6 – LOW SENSITIVITY SCAN), UDRPS DATA

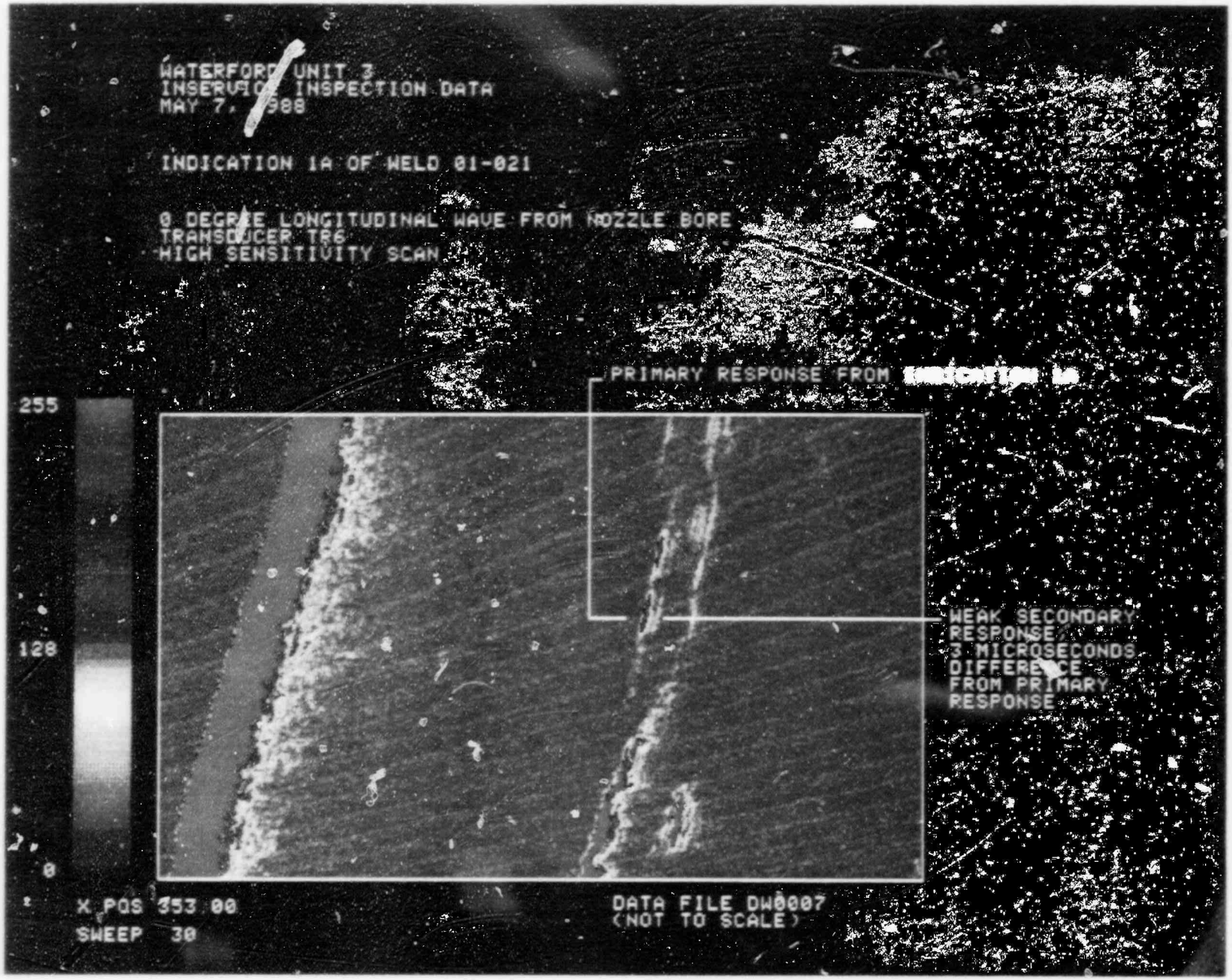

FIGURE A.12 : SECONDARY IMAGES OF INDICATION 1A (TRANSDUCER TR 6 – HIGH SENSITIVITY SCAN), UDRPS DATA – SWEEP WITH MAXIMUM AMPLITUDE FROM REFLECTOR

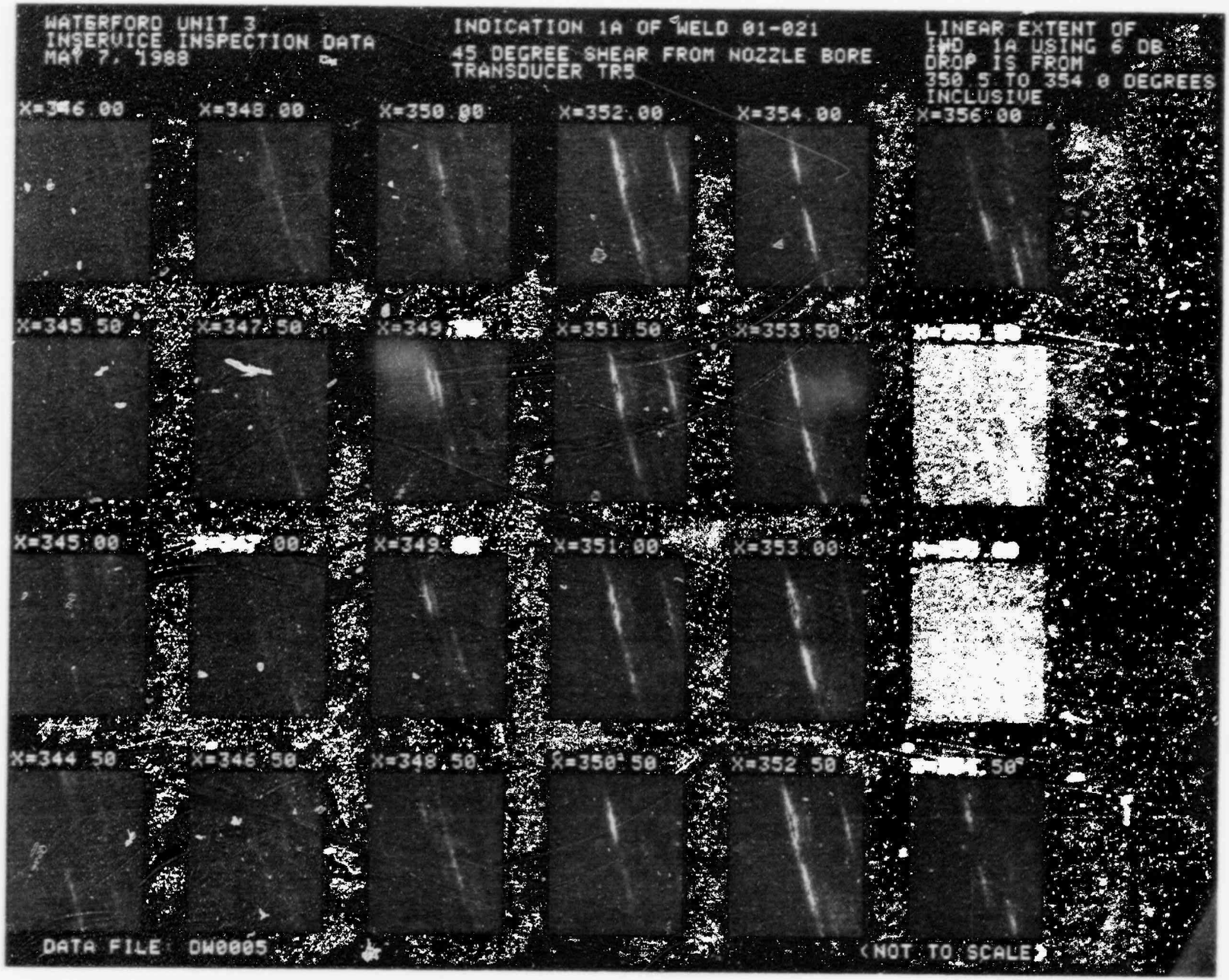

FIGURE A.13 : LINEAR EXTENT OF INDICATION 1A (TRANSDUCER TR 5 - LOW SENSITIVITY SCAN), UDRPS DATA

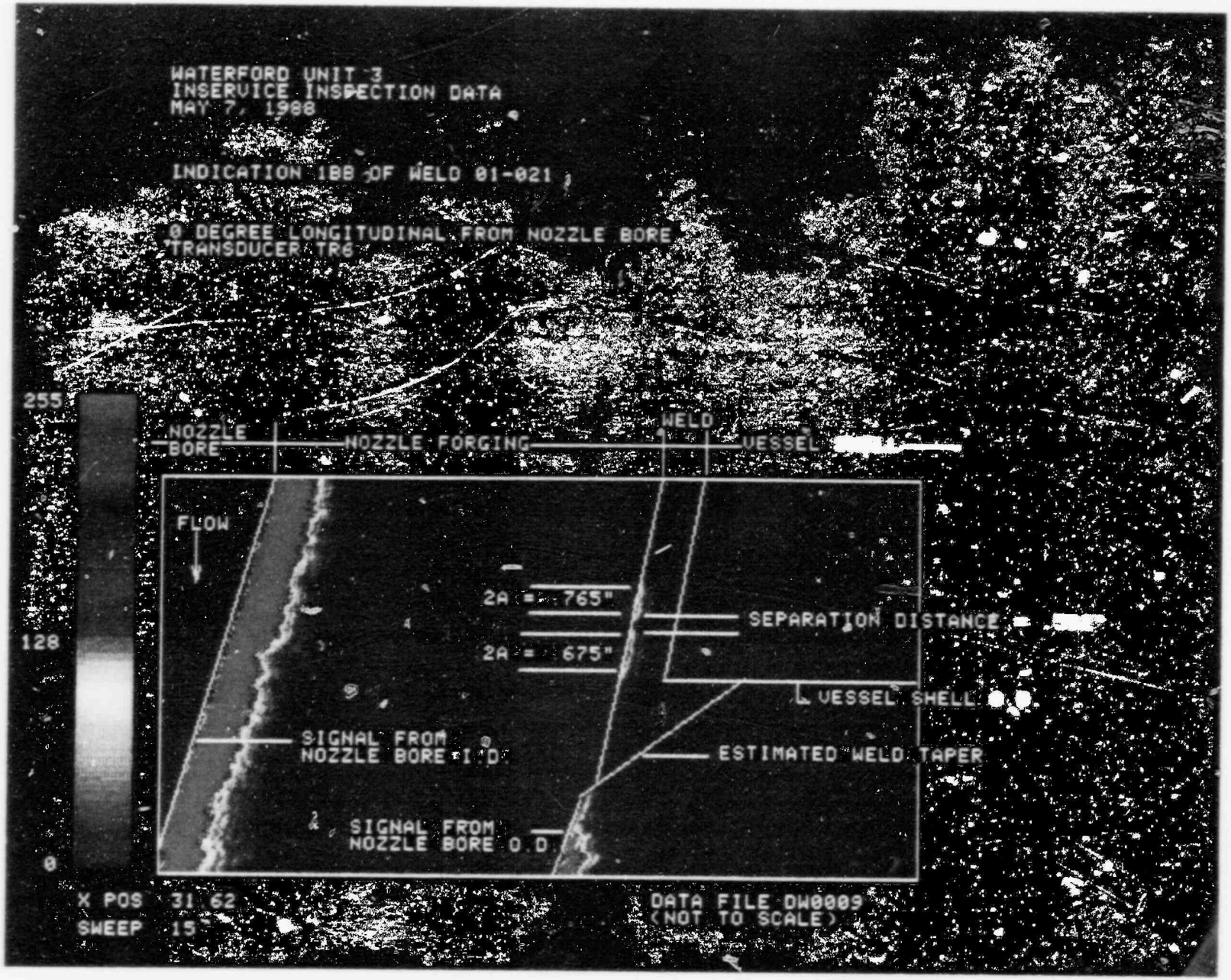

FIGURE A.14 : INDICATION 1BB IN OUTLET NOZZLE TO SHELL WELD 01-021 WITH RESPECT TO WELD CROSS-SECTION (TRANSDUCER TR 6 - LOW SENSITIVITY SCAN), UDRPS DATA - SWEEP WITH MAXIMUM AMPLITUDE FROM REFLECTOR

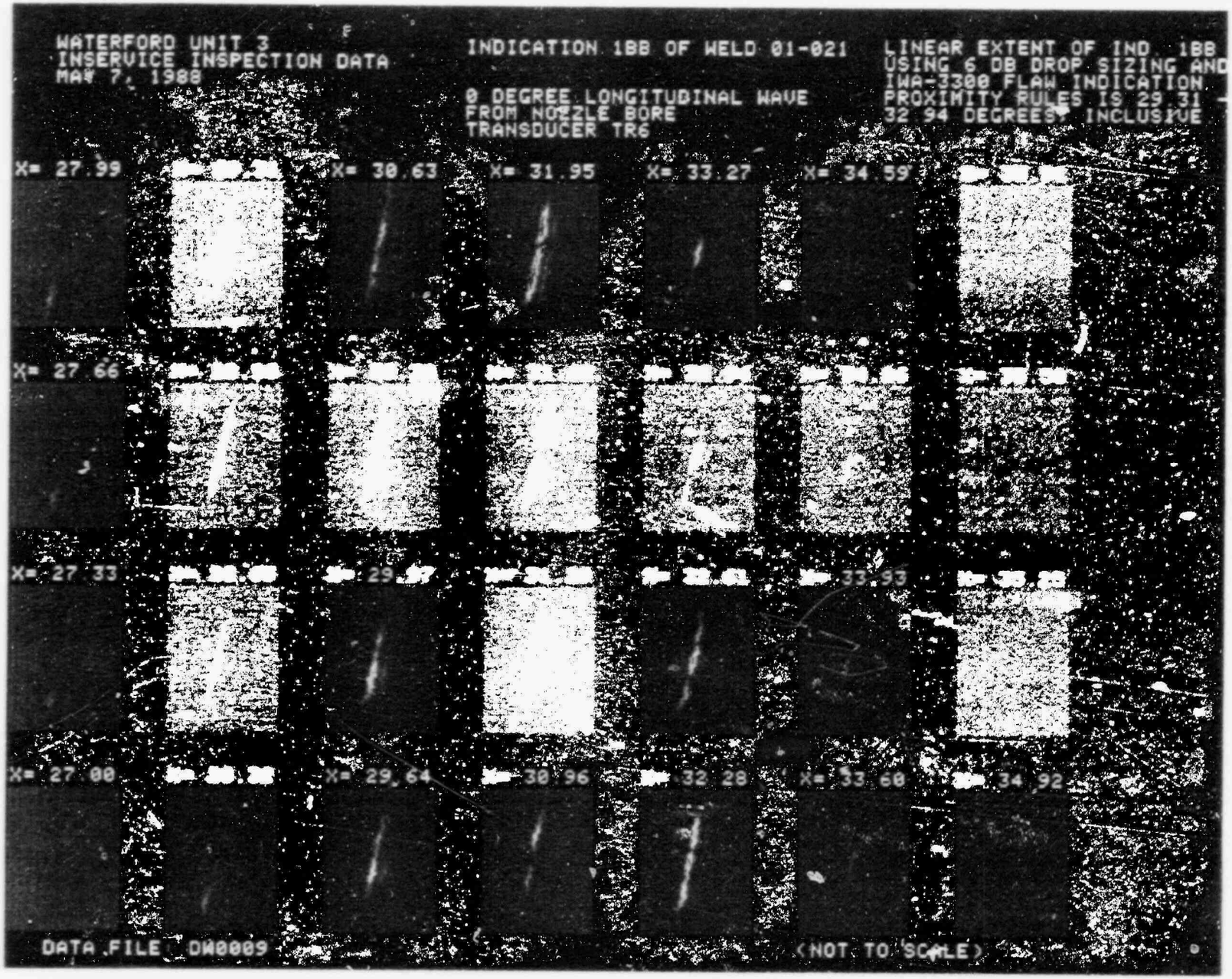

FIGURE A.15 : LINEAR EXTENT OF INDICATION 1BB (TRANSDUCER TR 6 - LOW SENSITIVITY SCAN), UDRPS DATA

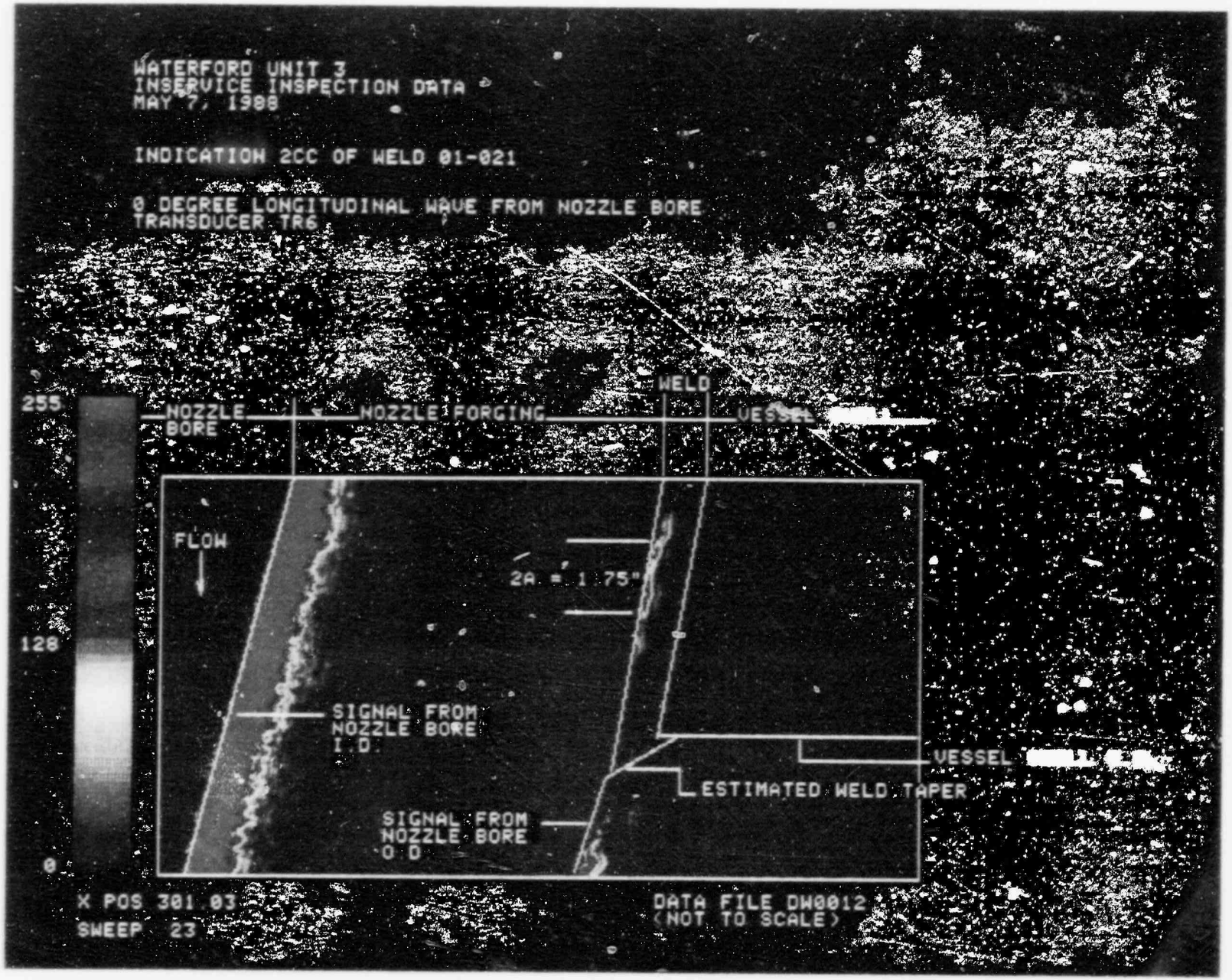

FIGURE A.16 : INDICATION 2CC IN OUTLET NOZZLE TO SHELL WELD 01-021 WITH RESPECT TO WELD CROSS-SECTION (TRANSDUCER TR 6 – LOW SENSITIVITY SCAN), UDRPS DATA – SWEEP WITH MAXIMUM AMPLITUDE FROM REFLECTOR

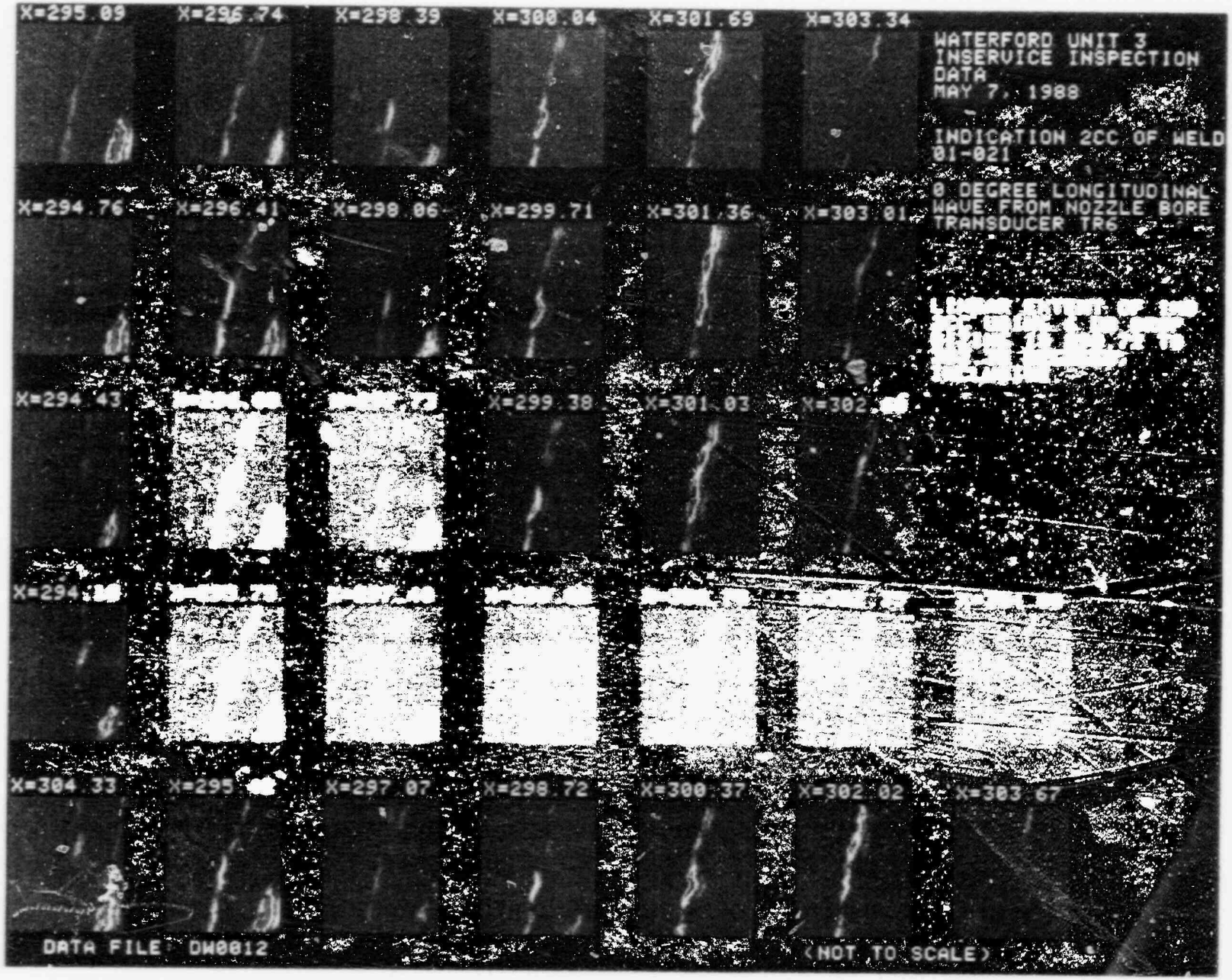

FIGURE A.17 : LINEAR EXTENT OF INDICATION 2CC (TRANSDUCER TR 6 – LOW SENSITIVITY SCAN), UDRPS DATA